

This is the peer reviewed version of the following article:

Effects of upgrading systems on energy conversion efficiency of a gasifier - fuel cell - gas turbine power plant / Pedrazzi, Simone; Allesina, Giulio; Tartarini, Paolo. - In: ENERGY CONVERSION AND MANAGEMENT. - ISSN 0196-8904. - 126:(2016), pp. 686-696. [10.1016/j.enconman.2016.08.048]

Terms of use:

The terms and conditions for the reuse of this version of the manuscript are specified in the publishing policy. For all terms of use and more information see the publisher's website.

10/04/2024 14:58

Manuscript Number: ECM-D-16-03320R1

Title: Effects of upgrading systems on energy conversion efficiency of a
gasifier - fuel cell - gas turbine power plant

Article Type: Original research paper

Section/Category: 3. Clean Energy and Sustainability

Keywords: Biomass; Gasification; Modeling; Solide Oxide Fuel Cells;
Zeolites; PPO membrane

Corresponding Author: Dr. Simone Pedrazzi, Ph.D.

Corresponding Author's Institution: University of Modena and Reggio
Emilia

First Author: Simone Pedrazzi, Ph.D.

Order of Authors: Simone Pedrazzi, Ph.D.; Giulio Allesina, Ph.D.; Paolo
Tartarini, Full professor

Abstract: This work focuses on a DG-SOFC-MGT (downdraft gasifier- solid oxide fuel cell - micro gas turbine) power plant for electrical energy production and investigates two possible performance-upgrading systems: polyphenylene oxide (PPO) membrane and zeolite filters. The first is used to produce oxygen-enriched air used in the reactor, while the latter separates the CO₂ content from the syngas. In order to prevent power plant shutdowns during the gasifier reactor scheduled maintenance, the system is equipped with a gas storage tank. The generation unit consists of a SOFC-MGT system characterized by higher electrical efficiency when compared to conventional power production technology (IC engines, ORC and EFGT). Poplar wood chips with 10% of total moisture are used as feedstock. Four different combinations with and without PPO and zeolite filtrations are simulated and discussed. One-year energy and power simulation were used as basis for comparison between all the cases analyzed. The modeling of the gasification reactions gives results consistent with literature about oxygen-enriched processes. Results showed that the highest electrical efficiency obtained is 32.81%. This value is reached by the power plant equipped only with PPO membrane filtration. Contrary to the PPO filtering, zeolite filtration does not increase the SOFC-MGT unit performance while it affects the energy balance with high auxiliary electrical consumption. This solution can be considered valuable only for future work coupling a CO₂ sequestration system to the power plant.



UNIVERSITÀ DEGLI STUDI
DI MODENA E REGGIO EMILIA

Department of Engineering "Enzo Ferrari"
University of Modena and Reggio Emilia
Via Vivarelli, 10/1 - 41125 Modena, Italy



BEE Lab (Bio Energy Efficiency Laboratory)
www.beelab.unimore.it

Dr. Simone Pedrazzi

Department of Engineering "Enzo Ferrari"
University of Modena and Reggio Emilia
Via Vivarelli, 10/1 – 41125 Modena, Italy
phone +39 059 205 6229, email: simone.pedrazzi@unimore.it

Professor Moh' Ahmad Al-Nimr

Editor-in-Chief
Energy Conversion and Management

Dear Professor Moh' Ahmad Al-Nimr:

I am pleased to submit an original research article entitled "**Effects of upgrading systems on energy conversion efficiency of a gasifier - fuel cell - gas turbine power plant**" by Simone Pedrazzi, Giulio Allesina and Paolo Tartarini for consideration for publication in the *Energy Conversion and Management* journal.

This work focuses on a downdraft gasifier- solid oxide fuel cell - micro gas turbine power plant for electrical energy production and investigates two possible performance-upgrading systems: polyphenylene oxide (PPO) membrane and zeolite filters. The first is used to produce oxygen-enriched air before the reactor, while the latter separates the CO₂ content from the syngas. In order to prevent power plant shutdowns during the gasifier reactor scheduled maintenance, the system is equipped with a gas storage tank. The generation unit consists of a SOFC-MGT system characterized by higher electrical efficiency when compared to conventional power production technology (IC engines, ORC and EFGT). Poplar wood chips with 10 % of total moisture are used as feedstock. Four different combinations with and without PPO and zeolite filtrations are simulated and discussed. One-year energy and power simulation were used as basis for comparison between all the cases analyzed. The modeling of the gasification reactions gives results consistent with literature about oxygen-enriched processes. Results shown that the highest electrical efficiency obtained is 32.81 %. This value is reached by the power plant equipped only with PPO membrane filtration. Contrary to the PPO filtering, zeolite filtration does not increase the SOFC-MGT unit performance while it affects the energy balance with high auxiliary electrical consumption. This solution can be considered valuable only for future work coupling a CO₂ sequestration system to the power plant.

Furthermore, with this letter the authors certify that the content of the paper and its novelty results are the original work of the authors and it was not submitted before in this journal. With this letter all the authors mutually agree to submit their manuscript to Energy Conversion and Management. If you felt that the manuscript is appropriate for your journal, we suggest the following reviewers:

- Prof. S. Dasappa, Faculty, Center for Sustainable Technologies, Indian Institute of Science;
- Dr. Pierluigi Leone, Department of Energy, Polytechnic University of Turin;



UNIVERSITÀ DEGLI STUDI
DI MODENA E REGGIO EMILIA

Department of Engineering "Enzo Ferrari"
University of Modena and Reggio Emilia
Via Vivarelli, 10/1 - 41125 Modena, Italy



BEE Lab (Bio Energy Efficiency Laboratory)
www.beelab.unimore.it

– Dr. Florian Monlau, APESA, Plateau Technique, France.

We look forward to hearing from you soon.

Best regards,

Dr. Simone Pedrazzi

Dr. Giulio Allesina

Pror. Paolo Tartarini

Highlights

- An advanced gasifier-SOFC-MGT system is modeled.
- An overall electrical efficiency of 32.81% is reached.
- Influence of all the sub-system modeled on the power plant efficiency is discussed.
- Compression storage of syngas is taken into account.

Effects of upgrading systems on energy conversion efficiency of a gasifier - fuel cell - gas turbine power plant

Simone Pedrazzi^{a,*}, Giulio Allesina^a, Paolo Tartarini^a

^a*University of Modena and Reggio Emilia, Department of Engineering 'Enzo Ferrari',
Via Vivarelli 10/1, 41125 Modena, Italy*

Abstract

THIS PAPER IS SUBMITTED WITH THE OPTION 'YOUR PAPER YOUR WAY'. FOR THIS REASON LAYOUT AND STYLE MAY DIFFER FROM THE JOURNAL ONE.

This work focuses on a DG-SOFC-MGT (downdraft gasifier- solid oxide fuel cell - micro gas turbine) power plant for electrical energy production and investigates two possible performance-upgrading systems: polyphenylene oxide (PPO) membrane and zeolite filters. The first is used to produce oxygen-enriched air used in the reactor, while the latter separates the CO_2 content from the syngas. In order to prevent power plant shutdowns during the gasifier reactor scheduled maintenance, the system is equipped with a gas storage tank. The generation unit consists of a SOFC-MGT system characterized by higher electrical efficiency when compared to conventional power production technology (IC engines, ORC and EFGT). Poplar wood chips with 10% of total moisture are used as feedstock. Four different combinations with and without PPO and zeolite filtrations are simulated and discussed. One-year

*Corresponding author

Email address: simone.pedrazzi@unimore.it (Simone Pedrazzi)

energy and power simulation were used as basis for comparison between all the cases analyzed. The modeling of the gasification reactions gives results consistent with literature about oxygen-enriched processes. Results showed that the highest electrical efficiency obtained is 32.81%. This value is reached by the power plant equipped only with PPO membrane filtration. Contrary to the PPO filtering, zeolite filtration does not increase the SOFC-MGT unit performance while it affects the energy balance with high auxiliary electrical consumption. This solution can be considered valuable only for future work coupling a CO_2 sequestration system to the power plant.

Keywords:

Biomass, Gasification, Modeling, Solide Oxide Fuel Cells, Zeolites, PPO membrane

1. Introduction

Due to the abundant availability and distribution, biomasses hold key-roles in plans for renewable energy production. This trend is becoming even more relevant thanks to the good degree of reliability and efficiency of the biomass-based technologies together with the high subsidies granted by several government for sustainable electrical energy production [1].

Depending on the feedstock quality and availability, biomasses are converted into energy through different technologies. In the case of ligno-cellulosic biomasses, a technology of great validity is gasification. This thermo-chemical process turns solid biomass into a gaseous fuel known as syngas, which can be converted into electrical energy through all those systems used for power production from gaseous fuels [2]. Gasification is today one of the most effi-

cient technologies to convert wood into electricity and it is also sustainable in terms of the environmental balance of CO_2 [3, 4].

Most of the gasification power plants use an IC engine-generator to convert the syngas chemical energy into electrical power. However, in some cases other conversion machines are used, i.e. Organic Rankine Cycles (ORC), External Firing Gas Turbines (EFGT)[5] and Stirling engines are used with the major advantage of having minor limitation about the syngas level of purification [2, 6, 7, 8, 9]. These systems are usually characterized by low conversion efficiencies of about 10-12%. Major conversion rates can be obtained only with electrochemical devices such as proton exchange membrane fuel cells [10], Molten Carbonate Fuel Cells (MCFC) [11, 12], Solid Oxide Fuel Cells (SOFC) [13, 14, 15], systems composed of SOFC and Micro Gas Turbines (MGT) [16, 17, 18, 19, 20, 21, 22, 23, 24, 25, 26] and systems composed of SOFC-MGT-ORC [27]. Despite the high rate of energy conversion, these systems require perfectly clean syngas [28]. Downdraft gasifiers are the most suitable architecture due to the low tar and particulate content in their gas when compared to updraft, crossdraft or fluidized bed gasifiers [2, 6, 29]. However, downdraft gasifiers commonly use air as gasification agent. This solution generates a syngas with a low calorific value where the hydrogen, methane and carbon monoxide are diluted in non-burnable gases: N_2 (about 50%) and CO_2 (from 10 to 20%). Otherwise, it is possible to choose oxygen gasification that produces a syngas with negligible N_2 content. However, oxygen gasification is a complex and expensive technology due to the gasification agent supply sub-systems and reactor material choice. Indeed, temperatures inside the reactor can reach 1200-1300 K when oxygen is used instead of air

38 [30].

39 The basic system discussed in this study is composed of an air blown-
40 downdraft-fixed bed gasifier fed with poplar wood chips. This work is aimed
41 at investigating the effects of different power plant designs on the overall
42 energy conversion efficiency.

43 The first power plant upgrading sub-system consists of a polyphenylene
44 oxide (PPO) membrane used to produce oxygen-enriched air. The gas sep-
45 aration characterization of this membrane is reported in literature [31, 32].
46 In practice, membrane gas separation is applied to increase the oxygen con-
47 tent in the inlet air of biomass boilers [33]. Bisio et al. studied the ther-
48 modynamics of combustion with enriched air and reviewed several types of
49 membranes [34]. Coombe and Nieh developed a membrane-based device for
50 air enrichment in small scale burners [35]. Hao et al. applied an oxygen-
51 permeable membrane to a reactor for the co-production of dimethyl ether
52 (DME)/methanol and electricity [36]. This paper uses PPO membrane in
53 order to obtain air with about 50% of oxygen then used as gasification agent.
54 This solution is a hybrid between air and pure oxygen gasification. Enriched
55 air reduces the reactor thermal stress compared to pure oxygen gasification,
56 while the syngas has a lower N_2 content than the one obtained in pure air
57 gasification. In addition, the syngas flow rate decreases because, for a fixed
58 power output, the enriched air flow required for gasification is lower than air
59 used in conventional gasification. This happens because the same amount of
60 oxygen is used in both cases and its concentration in enriched air is higher
61 than untreated air. Finally, the tar production is lower than air gasification
62 as consequence of the higher temperature that cracks more efficiently the

63 primary tars from pyrolysis [37].

64 A second solution discussed in this work consists of a porous media used
65 to upgrade the syngas. In fact, syngas has a variable CO_2 content depending
66 on gasification process as well as several boundary conditions. This value
67 ranges from 10% to 30% and it reduces significantly the higher heating value
68 of the syngas [37]. A solution to overcome this issue is to adopt a pressure-
69 swing selective synthetic zeolite filter. This system is placed before the gas
70 storage in order to separate carbon dioxide from syngas [38, 39]. The filter
71 can be constantly regenerated using a rotary valve packaged into modules
72 as described by Tagliabue et al. [40]. Literature investigation about zeolite
73 filtration outlines several works. Bacsik et al. studied the biogas CO_2-CH_4
74 separation through zeolites [41]. Kacem et al. investigated the pressure swing
75 adsorption for CO_2/N_2 and CO_2/CH_4 separation using activated carbon and
76 several types of zeolites [42]. Dirar et al. investigated intrinsic adsorption
77 properties of CO_2 on 5A and 13X zeolite [43].

78 The syngas obtained from gasification is stored and then used in a SOFC
79 unit able to produce electrical and thermal energy. The number of stacks
80 within the cell is optimized taking into account the optimal electrical cur-
81 rent density. The chosen number guarantees a good efficiency, however the
82 gas discharged from the cell still contains some chemical energy. For this
83 reason, this work suggests to convert this residual energy in a micro gas tur-
84 bine (MGT). The syngas storage allows the generation unit to operate in its
85 optimal point, furthermore it prevent the power plant shouting down dur-
86 ing the maintenance operations of the gasifier. This management preserves
87 the SOFC and MGT reliability. However, it is difficult to design the stor-

age capacity because an oversize storage rises the systems costs, while an undersized capacity reduces the time gained for the maintenance. For this reason, the storage was designed taking into account the tanks pressure, the electrical power production of the SOFC-MGT unit and the time required for scheduled stops of the gasifier for maintenance operations.

The mathematics of the whole system was developed starting from literature. The overall model has been implemented in Matlab SimulinkTM software environment in order to simulate the behavior of the system under different conditions over a year long simulation.

2. System modeling

The basic system layout is reported in Figure 1. The most relevant components are:

- **Downdraft gasifier:** The gasifier is equipped with a subsystem for the syngas filtering and cooling with water scrubber and electrostatic filters.
- **Syngas storage:** It consists of a tank of a total volume of 650 m³.
- **SOFC unit:** This subsystem consists of 10875 solid oxide cells and it is connected to the electrical grid by a power inverter.
- **Micro gas turbine (MGT):** this turbo-machinery is used to convert the last part of chemical energy content in the syngas purged by the SOFC.

109 This work investigates the effect of the implementation of the following
110 sub-systems to the basic scheme:

111 • **PPO membrane filter module:** The PPO sub-system consists of
112 the membrane filter and a compressor that increases the pressure of
113 the air before the PPO membrane filter to about 1 MPa. The oxygen
114 enriched air is sent to the gasifier at atmospheric pressure. A flow of
115 nitrogen is purged from the PPO module.

116 • **Zeolite (ZEO) filter module:** the zeolite (ZEO) filter module is
117 placed after the first syngas compressor. There is a further syngas
118 compression stage ahead the storage tanks because the ZEO module
119 works at 0.5 MPa of pressure as described in Section 2.3, while the
120 pressure in the storage is often higher.

121 The syngas is used as fuel in the SOFC stack. In this device, the fuel
122 reforming occurs at the anode and there is a recirculation of the 20% of
123 the anode exhaust to increase the fuel reforming performance [18, 22]. The
124 anode exhaust is used to preheat the syngas, then it is finally burned in the
125 MGT burner together with the cathode exhaust. The air required for the
126 electrochemical reaction is compressed and preheated in the recuperator of
127 the MGT as well as in the air preheater of the SOFC.

128 The SOFC stack generates DC current which is converted into AC current
129 by an inverter and it is sent to the electrical grid. The MGT drags the air
130 compressor and the remaining mechanical energy is converted into electrical
131 energy by an alternator.

132 2.1. PPO module modeling

133 Polymeric membranes allow to separate different gaseous components de-
 134 pending on the pore size and pressure applied to the filter [31]. In this work
 135 a membrane is used to separate nitrogen from air. The membranes widely
 136 used for this purpose are: Matrimid, Polyphenylenoxide (PPO) and Poly-
 137 dimethylsiloxan (PDMS) [31]. As showed in Figure 2, in membranes the
 138 inlet air flow is divided in permeate and retentate molar flows. The inlet
 139 flow (Q_{air} [mol/s]) has a pressure p_{feed} [atm] and it is composed of x_{O_2Feed}
 140 and x_{N_2Feed} molar fractions of oxygen and nitrogen. The permeate molar
 141 flow (Q_P [mol/s]) has a pressure $p_{permeate}$ [atm] and it is composed of y_{O_2}
 142 and y_{N_2} molar fractions of oxygen and nitrogen. The retentate molar flow
 143 (Q_R [mol/s]) has a pressure p_{feed} [atm] and it is composed of $x_{O_2Retentate}$ and
 144 $x_{N_2Retentate}$ molar fractions of oxygen and nitrogen.

145 Each membrane behavior is identified through two parameters: the selec-
 146 tivity (α) and the permeability to oxygen (γ). The first factor represents the
 147 attitude of the membrane to attract oxygen, the second quantifies the atti-
 148 tude of the membrane to be crossed by it. High selectivity and permeability
 149 ensure great filtering performance in terms of high value of y_{O_2} and a small
 150 membrane surface area is required to filter a given amount of air. Table 1
 151 presents the parameters of Matrimid, PPO and PDSM membranes.

152 The choice of a PPO membrane is a compromise in terms of acceptable
 153 values of selectivity and permeability. In order to simulate the behavior of
 154 the membranes, a mathematical model has been implemented from Melin
 155 and Rautenbach [31]. The model is based on the following assumptions:

- 156 • Air is considered a binary gas mixture with 21% oxygen and 79% ni-

157 trogen.

- 158 • Steady state conditions.
- 159 • Isotherm conditions.
- 160 • Isobaric conditions.
- 161 • Perfect gas law.
- 162 • Constant permeability.
- 163 • Perfect mixing conditions on upstream and downstream sides.
- 164 • Concentration polarization at the membrane is neglected.
- 165 • Pressure loss in the porous support layer is neglected.
- 166 • The permeate can drain off freely.

167 The calculation of the permeate composition is made with the following
168 formula taken from the work of Melin and Rautenbach [31]:

$$y_{O_2} = \frac{1}{2} \left[1 + \phi * \left(x_{O_2 Feed} + \frac{1}{\alpha - 1} \right) \right] - \sqrt{\left[\frac{1}{2} \left[1 + \phi * \left(x_{O_2 Feed} + \frac{1}{\alpha - 1} \right) \right] \right]^2 - \frac{\alpha * \phi * x_{O_2 Feed}}{\alpha - 1}} \quad (1)$$

$$y_{N_2} = 1 - y_{O_2} \quad (2)$$

169 where ϕ [-] is the feed-permeate pressure ratio given by the following
170 equation:

$$\phi = p_{feed}/p_{permeate} \quad (3)$$

Figure 3 reports the permeate composition over pressure ratio for the three membrane types considered. It can be seen that only a certain maximum of oxygen ratio can be achieved because all the graphs are leveling off. Therefore a pressure ratio of 1 MPa was chosen for further calculations as suggested in Melin and Rautenbach [31] and the $p_{retentate}$ was fixed at 1 atm.

The Matrimid membrane is able to produce the highest oxygen ratio of 0.58 % vol. in the permeate, however PPO membrane presents a good value of oxygen ratio (0.49 % vol.) and an acceptable value of permeability, therefore this membrane is adopted in the simulations. The active area of the membrane can be assessed from the molar flow of oxygen required for the gasification Q_{PO_2} [mol/s]:

$$A_{membrane} = \frac{Q_{PO_2}}{\gamma * (x_{O_2Feed} * p_{feed} + y_{O_2} * p_{permeate})} \quad (4)$$

The molar flow of nitrogen Q_{PN_2} [mol/s] and the total permeate molar flow Q_P [mol/s] is given by the following equations:

$$Q_{PN_2} = \frac{\gamma}{\alpha} * [p_{feed} * (1 - x_{O_2Feed}) + p_{permeate} * (1 - y_{O_2})] \quad (5)$$

$$Q_P = Q_{PN_2} + Q_{PO_2} \quad (6)$$

The molar flow of the inlet air Q_{air} , the retentate molar flow Q_R and the retentate composition ($x_{O_2Retentate}$ and $x_{N_2Retentate}$) are calculated setting to zero the amount of oxygen in the retentate flow as suggested by Melin and

187 Rautenbach[31]. Thus, a mass balance equation can be applied to estimate
 188 Q_{air} and Q_R :

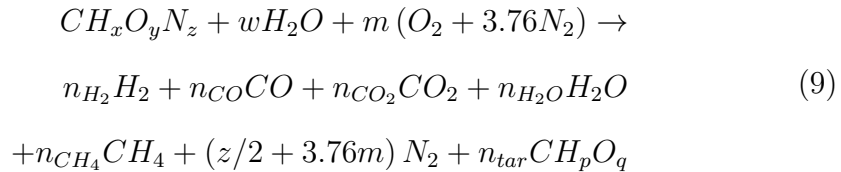
$$Q_{air} * x_{O_2 Feed} = Q_P * y_{O_2} \rightarrow Q_{air} = \frac{Q_P * y_{O_2}}{x_{O_2 Feed}} \quad (7)$$

$$Q_{air} = Q_P + Q_R \rightarrow Q_R = Q_{air} - Q_P \quad (8)$$

189 Finally, the electrical power consumption to pressurize the inlet air flow
 190 is calculated as a polytropic compression by Equation 15 assuming $T_{in} = 20$
 191 $^{\circ}C$; $m = 1.2$ and $\eta_{comp} = 90\%$.

192 2.2. Gasifier modeling

193 In this work, the gasification process is simulated using a black-box model
 194 based on Barman's work [44]. The model is validated for downdraft gasifiers;
 195 it is based on the following gasification equation:



196 where $CH_xO_yN_z$ is the equivalent chemical formula of "dry and ash
 197 free" (daf) biomass; CH_pO_q is the equivalent chemical formula of tar [45];
 198 w [mol/mol_{bio}] is the specific molar amount of the biomass moisture; m
 199 [mol/mol_{bio}] is the specific molar amount of oxygen calculated starting from
 200 the equivalence ratio ER as suggested by Jarungthammachote and Dutta[46];
 201 $n_{H_2}, n_{CO}, n_{CO_2}, n_{H_2O}, n_{CH_4}, n_{tar}$ [mol/mol_{bio}] are the specific molar amounts
 202 of $H_2, CO, CO_2, H_2O, CH_4$ and tar which constitute the syngas.

203 This model is used and discussed in several other works [47, 48, 49]. It
 204 consists of a chemical and a thermal sub-models that converge to the final
 205 composition of the gas. The first step is to choose an initial temperature T
 206 [K] and calculate the equilibrium constant of the following reactions:

- 207 • **K1:** Water-gas shift $CO + H_2O \leftrightarrow CO_2 + H_2$
- 208 • **K2:** Hydrogasification $C + 2H_2 \leftrightarrow CH_4$
- 209 • **K3:** Methane steam reforming $CH_4 + H_2O \leftrightarrow CO + 3H_2$

210 The system of equations 10 reported below is composed of three chemical
 211 balances calculated from Equation 9 (carbon, hydrogen and oxygen) and
 212 the three equilibrium constants for water-gas, hydrogasification and methane
 213 reforming reactions. The system is solved with the Newton-Raphson method.

$$\left\{ \begin{array}{l} n_{CO} + n_{CO_2} + n_{CH_4} + n_{tar} - 1 = 0 \\ 2n_{H_2} + 2n_{H_2O} + 4n_{CH_4} + pn_{tar} - x - 2w = 0 \\ n_{CO} + 2n_{CO_2} + n_{H_2O} + qn_{tar} - w - 2m - y = 0 \\ K_1 = \frac{n_{CO_2} * n_{H_2}}{n_{CO} * n_{H_2O}} \\ K_2 = \frac{n_{CH_4} * \frac{\dot{n}_{tot, wet}}{\dot{n}_{bio, daf}}}{n_{H_2}^2} \\ K_3 = \frac{n_{CO} * n_{H_2}^3}{\left(\frac{\dot{n}_{tot, wet}}{\dot{n}_{bio, daf}} \right)^2 n_{H_2O} n_{CH_4}} \end{array} \right. \quad (10)$$

214 Once the molar specific amounts of the syngas species are evaluated, it is
 215 possible to solve the thermodynamic energy balance of the system reported
 216 in the following equation:

$$\sum_{j=react} n_j * HF_j^0 = \sum_{i=prod} n_i * (HF_i^0 + \Delta H_{T,i}) \quad (11)$$

217 where n_j [moles] and HF_j^0 [kJ/kmol] are the specific moles amount and
 218 standard heat of formation of the j-th reagent (biomass, air and moisture); n_i
 219 [moles] and HF_i^0 [kJ/kmol] are the specific moles amount and the standard
 220 heat of formation of the i-th product (H_2 , CO , CO_2 , H_2O , CH_4 and N_2) and
 221 $\Delta H_{T,i}$ is the enthalpy difference between any given state and the standard
 222 state for the i-th product. $\Delta H_{T,i}$ can be calculated starting from the specific
 223 heat of the product:

$$\Delta H_{T,i} = \int_{298.15}^T C_p(T) dT = \left| aT + b\frac{T^2}{2} + c\frac{T^3}{3} + d\frac{T^4}{4} \right|_{298.15}^T \quad (12)$$

224 where the coefficient a,b,c and d are defined for each gas by Jarungtham-
 225 machote and Dutta[46]. In order to find the equilibrium temperature T_{new} ,
 226 the system is considered adiabatic and the the Newton-Raphson method is
 227 applied to the equations. If $abs(T - T_{new}) < 0.1$ K then the calculated equi-
 228 librium temperature and molar specific gases amounts are the final results;
 229 otherwise, a new iteration is done in order to satisfy the previous condi-
 230 tion. The model is implemented in Python and the input are the biomass
 231 equivalent molecule, the equivalence ratio ER and the initial temperature.
 232 The temperature input is used only as a starting point for the iterating
 233 system; after few cycles the temperature converges to the ones that satisfy
 234 both the chemical and thermal sub-systems. About the ER, a value of 0.335

is assumed. This value is consistent with air blown gasification parameters [50, 37] and it is confirmed by the low tar content in the syngas. Poplar wood chips properties and gasifier model parameters are summarized in Table 1.

2.3. ZEO module modeling

The zeolite filter is able to reduce the total syngas molar flow of about 20% - 30 % by the adsorption of CO_2 . Zeolite 5A is chosen because it has a great selectivity for carbon dioxide in comparison with the other gases that constitute syngas [38]. The gas adsorption in porous solids has been described by the Langmuir equation [38, 39]:

$$q_i = \frac{q_{mi} * B_i * p_i}{1 + \sum_{j=1}^n B_j * p_j} \quad (13)$$

where q_i [mmol/g] is the adsorbed amount of the component i ; q_{mi} [mmol/g] is the saturation adsorbed amount of the component i ; B_i [1/kPa] is the Langmuir constant of the component i ; p_i [kPa] is the equilibrium partial pressure of the component i ; B_j [1/kPa] is the Langmuir constant of the component j ; p_j [kPa] is the equilibrium partial pressure of the component j ; i and j are the gas species of the syngas. Table 1 reports the Langmuir constants and the saturation adsorbed amounts for Zeolite 5A, while Figure 4 depicts the adsorption trends of the syngas gases as function of pressure. It can be noted the high CO_2 selectivity of the zeolite in comparison with others gases.

The mass of zeolite required for adsorbing all the carbon dioxide of the syngas depends on the molar flow of the dry syngas, its CO_2 molar fraction and kinetic constant of adsorption. The ZEO filter module can be constantly regenerated using a rotary valve packaged into modules as described in [40].

257 The mass of zeolite that needs to be regenerated every cycle with duration
 258 of t_{cycle} can be calculated as follows:

$$m_{zeo} = t_{cycle} * \dot{n}_{DG} * \frac{1 + \sum_{j=1}^n B_j * p_j}{q_{m,CO_2} * B_{CO_2} * p_{ads} * x_{CO_2}} \quad (14)$$

259 where p_{ads} [kPa] is the total pressure of the syngas inside the ZEO filter.
 260 A constant temperature of the zeolite filter and of the inlet syngas of 303 K is
 261 assumed and the pressure of the inlet syngas is set to 500 kPa as suggested in
 262 [38, 39]. The cycling time of regeneration depends on kinetic CO_2 adsorption
 263 constant. In this study a plausible time of 60 seconds is assumed and future
 264 work will investigate this aspect. Zeolites adsorption generates heat, Ranjani
 265 et al. [51] suggests that 64-70 kJ are released for every mole of CO_2 adsorbed.
 266 This heat needs to be discharge by the ZEO module in order to keep the
 267 temperature constant at 303 K. In this preliminary study, no attention was
 268 paid to the ZEO module heat balance. Furthermore, the gas filtering sub-
 269 system considered in this work is based on the power plant described by
 270 Allesina et al. [50]. It was designed with the idea of coupling the gasifier with
 271 an internal combustion engine. Since the minimum presence of tars could
 272 negatively affect the performance of the zeolite adsorber, syngas purification
 273 unit should be properly designed. A potential alternative to water scrubber
 274 is oil scrubber with subsequent stripping of tars [52, 53].

275 *2.4. Compressor and storage system modeling*

276 The modeling of the syngas compression is carried out considering it as
 277 a polytropic transformation. The electrical power required for compression
 278 is given by Pedrazzi et al. [54]:

$$P_{comp} = \frac{\dot{n}_{gas} L_{comp, is}}{\eta_{comp}} = \frac{\dot{n}_{gas}}{\eta_{comp}} \frac{z R T_{in}}{z - 1} \left[1 - \left(\frac{p_{out}}{p_{in}} \right)^{\frac{z-1}{z}} \right] \quad (15)$$

where z is the polytrophic coefficient, R is the universal gas constant equal to $8.314 \text{ J mol}^{-1} \text{ K}^{-1}$, T_{in} is the gas inlet temperature (25°C for syngas compressor 1 and 30°C for syngas compressor 2), p_{in} and p_{out} [atm] are the gas inlet and outlet pressures, \dot{n}_{gas} [mol/s] is the gas molar flow and η_{comp} is the compressor efficiency available from manufacturer's data [54]. The maximum pressure value inside the storage system is a fundamental parameter required to design the tanks and the compressor properly. Assuming ideal gas and a constant syngas storage temperature $T_s = 25^\circ\text{C}$, the pressure inside the tanks is calculated by the ideal gas law:

$$p_s = \frac{n R T_s}{V} \quad (16)$$

where n [mol] are the moles of syngas inside the tanks and V [m^3] is the storage total volume. Assuming a value of the initial syngas moles n_{in} inside the storage, the moles of syngas at the time τ [s] are given by:

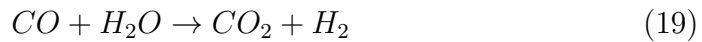
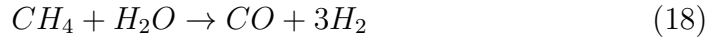
$$n = n_{in} + \int_0^\tau (\dot{n}_{in,s}(t) - \dot{n}_{out,s}(s)) dt \quad (17)$$

where $\dot{n}_{in,s}(t)$ and $\dot{n}_{out,s}(t)$ [mol/s] are the inlet and the outlet molar flow at the instantaneous time t [s]. Table 2 reports the model parameters of the storage and compressor sub-systems. The total volume of storage and the initial syngas amount in the tank are reduced of about 50% in comparison with the conventional system without PPO and ZEO modules as investigated in [55, 56]. This result is reached thanks to the PPO adoption that decreases

the molar flow of dry syngas of about the 20% - 30%, while the filtration in the ZEO module further reduces the syngas molar flow of about another 20% - 30% as shown in the results.

2.5. SOFC modeling

The SOFC model used in this study is based on the work of Bang-Møller and Rokni [18]. This model does not take into account the recirculation of gas at the cell anode. This feature may strongly compromise the fuel cell efficiency in case of the presence of gases that do not take part in the electro-chemical, shift and reforming reactions. Unfortunately, syngas contains considerable amounts of CO_2 and N_2 . To overcome this issue, the model previously cited is implemented with the reforming model presented by Rami Salah El-Emam et al. [22]. As described by Rami Salah El-Emam, the electro-chemical reactions take place in both the anode and the cathode of the cell (Eq.22), while the reforming and the monoxide water shift occur only near the anode (Eqs. 18, 19). Equation 22 presents the overall electro-chemical reaction that is divided into two sub-reactions: the hydrogen reacts with the oxygen ions to form water and electrons according to Eq. 20 at the anode, while, at the cathode, the oxygen from inlet air reacts with the electrons from the anode (Eq. 21) to form oxygen ions that flow to the anode through the solid oxide electrolyte.





317 The mathematical modeling of reforming and electrochemical reactions
 318 is explained in References [22] and [18]. Using these models, it is possible
 319 to calculate the electrical power production and the electrical conversion
 320 efficiency for a given syngas inlet flow with a specific composition. The
 321 SOFC model parameters adopted in the simulations are reported in Table 2.

322 2.6. MGT modeling

323 Mathematical description of gas turbines is well described in literature.
 324 Details and assumptions of the present model can be found in Bang-Møller
 325 and Rokni work [18]. Characteristics of the turbine and others components
 326 connected to the MGT are listed in Table 2.

327 3. Simulation results and discussion

328 In this work four different cases are simulated. First of all, the basic
 329 system composed of a downdraft gasifier, a storage tank and a SOFC-MGT
 330 is simulated. After this step, the two possible solutions consisting of N_2
 331 purging from air or CO_2 separation from syngas are discussed separately.
 332 Finally, the complete system provided with PPO module and ZEO module
 333 is simulated.

334 3.1. Case I (*Gasifier + SOFC + MGT*)

335 The SOFC-MGT unit constantly produces energy all over the year of
 336 simulation in order to preserve the stability of the cells and their gaskets,
 337 which are very sensitive to thermal stresses [57]. The syngas molar flow con-
 338 sumed by the SOFC-MGT unit is calculated by Equation 23 that considers
 339 the cycling working of the DG:

$$\dot{n}_{syngas-SOFC} = \frac{h_{operation}\dot{n}_{DG}}{h_{operation} + h_{maintenance}} \quad (23)$$

340

341 Figure 5 depicts the overall model implemented in Matlab SimulinkTM soft-
 342 ware environment. Table 3 reports the simulation results. Gasifier cold
 343 efficiency is about 79%, this value is confirmed by literature that suggests
 344 an efficiency of 70% - 80% for air-blown downdraft gasifier [37, 4, 44]. Syn-
 345 gas composition consists of about 19% vol. of H_2 and 15% vol. of CO , the
 346 higher heating value of 4.75 MJ/Nm³ is similar to the results reported by
 347 Basu [37] for this kind of gasifier. SOFC-MGT unit has a constant electrical
 348 power production of 197.43 kW all over the simulated year. The auxiliary
 349 consumption of the whole system strongly depends on tank pressurization
 350 level. The average annual value is 34.24 kW. For this reason, the net average
 351 power production is reduced to 163.19 kW and the electrical efficiency of the
 352 system is 25.43%.

353 3.2. Case II (*PPO + Gasifier + SOFC + MGT*)

354 Table 4 shows the results of the simulation of the system previously de-
 355 scribed and now equipped with the PPO module. The oxygen enriched air

356 flow is about 1.27 mol/s. This value is lower than 2.94 mol/s obtained with-
 357 out PPO membrane (Case I). Syngas composition is consistent with the work
 358 of Wang et al. [58], where oxygen-enriched air (50% oxygen and 50% nitro-
 359 gen) is used as gasifying agent in a double stage downdraft gasifier fueled
 360 with pine sawdust pellets. Differences of 1-2% between the model outputs
 361 and Wang's results about CO and H_2 contents are achieved (29% vs. 27%
 362 for H_2 and 26% Vs. 25% for CO). The gasification with oxygen-enriched air
 363 assures high gasifier performance in terms of cold gas efficiency (92%), tar
 364 production (0.27 g/Nm³) and syngas higher heating value (7.55 MJ/Nm³).
 365 The syngas outlet flow is 3.589 mol/s, consistently lower than Case I where
 366 syngas flow is 5.01 mol/s. The average equilibrium temperature of gasifi-
 367 cation in this case is 931 K. This value is only 36 K higher than Case I.
 368 Wang et al.[58] suggestes a peak temperature of about 1200 K with oxygen-
 369 enriched air. With this temperature, conventional material adopted in air
 370 gasifier can be used (i.e. stainless steel and refractory brick [2, 6]). In Case
 371 II, the overall net power production is 210.52 kW and the electrical efficiency
 372 is boosted to 32.81%. The average auxiliary consumption is 42 kW, 8 kW
 373 higher than Case I. This is due to the PPO module that uses air at 1 MPa
 374 pressure generated by an air compressor. The electrical consumption of the
 375 air compressor is 15.3 kW and it is fully compensated by the increasing of
 376 the gasifier efficiency and the SOFC-MGT unit efficiency.

377 3.3. Case III (*Gasifier + ZEO + SOFC + MGT*)

378 Table 5 resumes the simulation results of the system with the ZEO fil-
 379 tering module instead of PPO membrane. The filtered syngas has a higher
 380 heating value of 5.9 MJ/Nm³. This value falls between Case I (4.75 MJ/Nm³)

381 and Case II (7.55 MJ/Nm³). The pressure of the storage tank ranges between
 382 0.267-0.488 MPa, similar to the values obtained in Case II (0.266-0.462 MPa)
 383 and Case I (0.267-0.539 MPa). The zeolite mass required to perform con-
 384 tinuously the filtration is 23.742 kg. The value obtained is consistent with
 385 Tagliabue et al. work [40]. However, in future work, the CO_2 adsorbed by
 386 the ZEO module can be stored in order to create a carbon sequestration sys-
 387 tem. The power production and the net electrical efficiency of the system is
 388 low (148.74 kW of power production and 22.87% of electrical efficiency) as a
 389 consequence of the energy absorbed by the syngas compressor 1 (see Figure
 390 1) to increase the pressure of the syngas to 0.5 MPa before the ZEO module.
 391 This electrical energy consumption is higher than Cases II and I, in addition
 392 the efficiency of the SOFC-MGT module fueled with the filtered syngas is
 393 lower. As shown in Table 5, the SOFC-MGT efficiency in Case III is about
 394 34%, thus lower than Case II (42.08%) and Case I (37.46%).

395 3.4. Case IV (PPO + Gasifier + ZEO + SOFC + MGT)

396 The results about the fully equipped gasifier power system are reported
 397 in Table 6. A high power production (194.53 kW) and electrical efficiency
 398 (30.32%) is reached thanks to the high H_2 and CO amounts in the filtered
 399 syngas. In fact, the H_2 volume percentange reaches 41.53% and the CO
 400 volume percentange is boosted to 32.54%. As a consequence of this com-
 401 position, the higher heating value of the syngas is 10.19 MJ/Nm³, a value
 402 typical for oxygen-blown gasifiers [37]. Therefore, the SOFC-MGT unit syn-
 403 gas consumption is 2.696 mol/s. This value is about 45% lower than Case I
 404 (4.95 mol/s), 24% lower than Case II (3.545 mol/s) and 33% lower than Case
 405 III (4.02 mol/s). A pressure range of 0.266-0.415 MPa is achieved. In this

case power production and efficiency is lower than Case II as result of higher average auxiliary consumption (51.80 kW) and lower SOFC-MGT unit efficiency (38.41%). However, the utilization of the ZEO module has several advantages: separates the CO_2 and reduces the storage peaks pressure.

3.5. Performance and energy considerations

Figure 6 shows the electrical efficiency and the average power production in every scenario. Case II resulted the best in terms of energy conversion; the overall electrical efficiency reaches 32% and the power production is about 210 kW. These values are higher than commercial gasification power systems with internal combustion engines where the maximum electrical efficiency hardly reaches 25% [37, 4, 2]. This result is given by the PPO module that increases the gasifier efficiency to 92% (75% is the reference value for air blown gasifier [37]) and the SOFC-MGT module which has a higher electrical conversion efficiency (about 42%) compared to common engine-alternator generator units (about 27% [4, 59, 3]). Case II is the best in terms of energy balance as shown in Figure 7. These graphs do not consider the thermal energy that can be recovered from the gasifier or the SOFC-MGT unit. The highest energy loss occurs at the SOFC-MGT unit (about 52%), while auxiliary consumption of the blowers and the auxiliary equipment of the gasifier are low (9%). In Cases I and III, the low efficiency of the gasifier reduces the overall electrical performance of the system. In Cases III and IV the ZEO module consumes energy to separate the CO_2 from the gas, however no efficiency increase occurs in the SOFC-MGT unit with a CO_2 free syngas and the final result is a lower power production. The system modeled in this work is obtained starting from a reference power plant described by Allesina et. al

[50] where IC engines are used instead of the SOFC-MGT unit. The author reports an experimental cold gasification efficiency of 67%. Considering an electrical IC engine-alternator unit efficiency of about 27%, as suggested by Puglia et al. [3], the total electrical efficiency is about 18%. This value is 30% lower than Case I and it is 45% lower than Case II. Another study made by Patuzzi et al. [60] reports the values of the net electrical efficiency of three different commercial biomass gasifier - IC engine power plants. The average efficiency is about 20%, this value is consistent with the one obtained for Allesina et al. [50].

4. Conclusions

The biomass fueled system with PPO module (Case II) shows the higher electrical efficiency of about 33%. The reasons behind this result are various. First of all, oxygen-enriched air boosts the gasifier cold efficiency from 79% (Case I with air) to 92% (Cases II and IV with oxygen-enriched air). In addition, the SOFC-MGT unit presents a higher efficiency (about 42%) compared to IC engine-alternator unit (about 27%), ORC cycle (about 20%) or EFGT cycle (about 20%). In Cases III and IV, the zeolites adsorption module consumes energy to increase the higher heating value of the syngas but not the performance of the SOFC-MGT system, this reduces the overall system efficiency. The energy balances of four cases investigated show that the greater losses are in the SOFC-MGT unit. This unit has the difficult task to convert the chemical energy of a gas fuel into electrical energy in an efficient way. An efficiency of about 50% is reached with natural gas, in this study the maximum electrical efficiency is about 42% using a syngas

455 produced with an oxygen-enriched air as gasifying agent. This difference is
 456 given by the presence of several inert gases into the syngas that reduces the
 457 electrochemical conversion of the SOFC. The removal or the conversion of
 458 these gases into syntethic natural gases (SNG) is possible and, in this way,
 459 the efficiency of the SOFC-MGT unit will be similar to the value reach for
 460 natural gas one. But, cost and energy self-consumption of the upgrading
 461 process are very high and not convenient for this kind of power plants. Cases
 462 III and IV has a lower efficiency compared to Case II, however, with the
 463 ZEO module, it is possible to sepearate the CO_2 content of the syngas with
 464 environmental benefits in case the module is coupled with a CO_2 sequestra-
 465 tion system. Future work will consider exergy calculations and experimental
 466 tests on a micro-scale power system (5-20 kW of electrical power) with PPO
 467 module and SOFC module in order to validate modeling results and to assest
 468 system durability. In addition, economical net present value analysis will be
 469 done to estimate the economic sustainability of the power plant.

470 References

- 471 [1] IEA. Technology roadmap - bioenergy for heat and power. Technical
 472 report, IEA, 2012.
- 473 [2] Thomas B. Reed and Agua Das. *Handbook of Biomass Downdraft Gasi-*
 474 *fier Engine Systems*. The biomass energy foundation press, 1988.
- 475 [3] G. Allesina, S. Pedrazzi M.Puglia, and P. Tartarini. Upgrading or sub-
 476 stituting the gasification process for electrical energy production: an
 477 energy-based comparison. In *XXX UIT Conference, Bologna 2012*, 2012.

- 478 [4] H.A.M. Knoef. *Handbook of Biomass Gasification*. BTG, 2005.
- 479 [5] Amitava Datta, Ranjan Ganguly, and Luna Sarkar. Energy and exergy
480 analyses of an externally fired gas turbine (efgt) cycle integrated with
481 biomass gasifier for distributed power generation. *Energy*, 35(1):341 –
482 350, 2010.
- 483 [6] FAO Forestry Department Mechanical Wood Products Branch. *Woodgas
484 as engine fuel*, volume ISBN 92-5-102436-7. F.A.O., 1986.
- 485 [7] F. Martelli, G. Riccio, S. Maltagliati, and D. Chiaramonti. Technical
486 study and environmental impact of an external fired gas turbine power
487 plant fed by solid fuel. *1st world Conference of Biomass, Sevilla*, 2000.
- 488 [8] V. Naso. *La macchina di Stirling*. CEA, 1991.
- 489 [9] C. Souleymane. Motori a combustione interna e turbine a gas di pic-
490 cola taglia per gas di sintesi. Master’s thesis, Università degli Studi di
491 Padova, Italy., 2012.
- 492 [10] Farqad Al-Hadeethi, Moh’d Al-Nimr, and Mohammad Al-Safadi. Us-
493 ing the multiple regression analysis with respect to {ANOVA} and 3d
494 mapping to model the actual performance of {PEM} (proton exchange
495 membrane) fuel cell at various operating conditions. *Energy*, 90, Part
496 1:475 – 482, 2015.
- 497 [11] Guido Galeno. *Modellizzazione di un micro cogeneratore basato sulla
498 tecnologia mcfc accoppiata ad un gassificatore di biomassa*. PhD thesis,
499 University of Cassino, Italy, 2006-2007.

- [12] Giulio Donolo, Giulio De Simon, and Maurizio Fermeglia. Steady state simulation of energy production from biomass by molten carbonate fuel cells. *Journal of Power Sources*, 158(2):1282 – 1289, 2006. Special issue including selected papers from the 6th International Conference on Lead-Acid Batteries (LABAT 2005, Varna, Bulgaria) and the 11th Asian Battery Conference (11 ABC, Ho Chi Minh City, Vietnam) together with regular papers.
- [13] Stefano Cordiner, Massimo Feola, Vincenzo Mulone, and Fabio Romanelli. Analysis of a {SOFC} energy generation system fuelled with biomass reformat. *Applied Thermal Engineering*, 27(4):738 – 747, 2007. Energy: Production, Distribution and Conservation.
- [14] E. Achenbach. Three-dimensional and time-dependent simulation of a planar solid oxide fuel cell stack. *Journal of Power Sources*, 49:333–348, 1994.
- [15] M. Mortazaei and M. Rahimi. A comparison between two methods of generating power, heat and refrigeration via biomass based solid oxide fuel cell: A thermodynamic and environmental analysis. *Energy Conversion and Management*, 126:132 – 141, 2016.
- [16] F. Calise, M. Dentice d’Accadia, A. Palombo, and L. Vanoli. Simulation and exergy analysis of a hybrid solid oxide fuel cell (sofc)–gas turbine system. *Energy*, 31(15):3278 – 3299, 2006. {ECOS} 2004 - 17th International Conference on Efficiency, Costs, Optimization, Simulation, and Environmental Impact of Energy on Process Systems 17th Interna-

- 523 tional Conference on Efficiency, Costs, Optimization, Simulation, and
524 Environmental Impact of Energy on Process Systems.
- 525 [17] L. Fryda, K.D. Panopoulos, and E. Kakaras. Integrated {CHP} with
526 autothermal biomass gasification and sofc-mgt. *Energy Conversion and*
527 *Management*, 49(2):281 – 290, 2008.
- 528 [18] C. Bang-Moller and M. Rokni. Thermodynamic performance study of
529 biomass gasification, solid oxide fuel cell and micro gas turbine hybrid
530 systems. *Energy Conversion and Management*, 51(11):2330 – 2339, 2010.
- 531 [19] Made Sucipta, Shinji Kimijima, and Kenjiro Suzuki. Performance anal-
532 ysis of the sofc-mgt hybrid system with gasified biomass fuel. *Journal*
533 *of Power Sources*, 174(1):124 – 135, 2007. jce:titleHybrid Electric Ve-
534 hiclesj/ce:title.
- 535 [20] Pegah Ghanbari Bavarsad. Energy and exergy analysis of internal re-
536 forming solid oxide fuel cell“gas turbine hybrid system. *International*
537 *Journal of Hydrogen Energy*, 32(17):4591 – 4599, 2007. Fuel Cells.
- 538 [21] C. Ozgur Colpan, Ibrahim Dincer, and Feridun Hamdullahpur. Thermo-
539 dynamic modeling of direct internal reforming solid oxide fuel cells oper-
540 ating with syngas. *International Journal of Hydrogen Energy*, 32(7):787
541 – 795, 2007. jce:titleFuel Cellsj/ce:title.
- 542 [22] Rami Salah El-Emam, Ibrahim Dincer, and Greg F. Naterer. Energy
543 and exergy analyses of an integrated {SOFC} and coal gasification sys-
544 tem. *International Journal of Hydrogen Energy*, 37(2):1689 – 1697, 2012.
545 jce:title10th International Conference on Clean Energy 2010j/ce:title.

- [23] Penyarat Chinda and Pascal Brault. The hybrid solid oxide fuel cell (sofc) and gas turbine (gt) systems steady state modeling. *International Journal of Hydrogen Energy*, 37(11):9237 – 9248, 2012.
- [24] S.H. Chan, H.K. Ho, and Y. Tian. Modelling of simple hybrid solid oxide fuel cell and gas turbine power plant. *Journal of Power Sources*, 109(1):111 – 120, 2002.
- [25] Tae Won Song, Jeong Lak Sohn, Jae Hwan Kim, Tong Seop Kim, Sung Tack Ro, and Kenjiro Suzuki. Performance analysis of a tubular solid oxide fuel cell/micro gas turbine hybrid power system based on a quasi-two dimensional model. *Journal of Power Sources*, 142(1â“2):30 – 42, 2005.
- [26] Mahsa Aghaie, Mehdi Mehrpooya, and Fathollah Pourfayaz. Introducing an integrated chemical looping hydrogen production, inherent carbon capture and solid oxide fuel cell biomass fueled power plant process configuration. *Energy Conversion and Management*, 124:141 – 154, 2016.
- [27] Masood Ebrahimi and Iraj Moradpoor. Combined solid oxide fuel cell, micro-gas turbine and organic rankine cycle for power generation (sofc-mgt-orc). *Energy Conversion and Management*, 116:120 – 133, 2016.
- [28] Ph. Hofmann, K.D. Panopoulos, P.V. Aravind, M. Siedlecki, A. Schweiger, J. Karl, J.P. Ouweltjes, and E. Kakaras. Operation of solid oxide fuel cell on biomass product gas with tar levels $\geq 10 \text{ g nm}^{-3}$. *International Journal of Hydrogen Energy*, 34(22):9203 – 9212, 2009.

- 569 [29] Lopamudra Devi, Krzysztof J Ptasinski, and Frans J.J.G Janssen. A re-
570 view of the primary measures for tar elimination in biomass gasification
571 processes. *Biomass and Bioenergy*, 24(2):125–140, 2003.
- 572 [30] Jinsong Zhou, Qing Chen, Hui Zhao, Xiaowei Cao, Qinfeng Mei,
573 Zhongyang Luo, and Kefa Cen. Biomass–oxygen gasification in a high-
574 temperature entrained-flow gasifier. *Biotechnology Advances*, 27(5):606
575 – 611, 2009. Bioenergy Research & Development in ChinaICBT
576 2008.
- 577 [31] T. Melin and R. Rautenbach. *Membranverfahren, Grundlagen der*
578 *Modul- und Anlagenauslegung*. 2007.
- 579 [32] K.C. Khulbe, T. Matsuura, G. Lamarche, and H.J. Kim. The morphol-
580 ogy characterisation and performance of dense ppo membranes for gas
581 separation. *Journal of Membrane Science*, 135(2):211 – 223, 1997.
- 582 [33] Janusz Kotowicz and Adrian Balicki. Enhancing the overall efficiency
583 of a lignite-fired oxyfuel power plant with {CFB} boiler and membrane-
584 based air separation unit. *Energy Conversion and Management*, 80:20
585 – 31, 2014.
- 586 [34] Giacomo Bisio, Alessandro Bosio, and Giuseppe Rubatto. Thermody-
587 namics applied to oxygen enrichment of combustion air. *Energy Con-*
588 *version and Management*, 43(18):2589 – 2600, 2002.
- 589 [35] H. Scott Coombe and Sen Nieh. Polymer membrane air separation per-
590 formance for portable oxygen enriched combustion applications. *Energy*
591 *Conversion and Management*, 48(5):1499 – 1505, 2007.

- [36] Yanhong Hao, Yi Huang, Minhui Gong, Wenying Li, Jie Feng, and Qun Yi. A polygeneration from a dual-gas partial catalytic oxidation coupling with an oxygen-permeable membrane reactor. *Energy Conversion and Management*, 106:466 – 478, 2015.
- [37] Prabir Basu. *Biomass Gasification and Pyrolysis: Practical Design and Theory*. Academic Press, Elsevier, 2010.
- [38] Saeed Pakseresht, Mohammad Kazemeini, and Mohammad M. Akbarnejad. Equilibrium isotherms for co, co₂, {CH₄} and {C₂H₄} on the 5a molecular sieve by a simple volumetric apparatus. *Separation and Purification Technology*, 28(1):53 – 60, 2002.
- [39] Gi-Moon Nam, Byung-Man Jeong, Seok-Hyun Kang, Byung-Kwon Lee, and Dae-Ki Choi. Equilibrium isotherms of ch₄, c₂h₆, c₂h₄, n₂, and h₂ on zeolite 5a using a static volumetric method. *Journal of Chemical & Engineering Data*, 50(1):72–76, 2005.
- [40] Marco Tagliabue, David Farrusseng, Susana Valencia, Sonia Aguado, Ugo Ravon, Caterina Rizzo, Avelino Corma, and Claude Mirodatos. Natural gas treating by selective adsorption: Material science and chemical engineering interplay. *Chemical Engineering Journal*, 155(3):553 – 566, 2009.
- [41] Zoltán Bacsik, Ocean Cheung, Petr Vasiliev, and Niklas Hedin. Selective separation of {CO₂} and {CH₄} for biogas upgrading on zeolite naka and sapo-56. *Applied Energy*, 162:613 – 621, 2016.

- 614 [42] Mariem Kacem, Mario Pellerano, and Arnaud Delebarre. Pressure swing
615 adsorption for CO_2/N_2 and CO_2/CH_4 separation: Comparison between ac-
616 tivated carbons and zeolites performances. *Fuel Processing Technology*,
617 138:271 – 283, 2015.
- 618 [43] Qassim Hassan Dirar and Kevin F. Loughlin. Intrinsic adsorption prop-
619 erties of CO_2 on 5a and 13x zeolite. *Adsorption*, 19(6):1149–1163, 2013.
- 620 [44] Niladri Sekhar Barman, Sudip Ghosh, and Sudipta De. Gasification of
621 biomass in a fixed bed downdraft gasifier – a realistic model including
622 tar. *Bioresource Technology*, 107:505–511, 2012.
- 623 [45] Takashi Yamazaki, Hirokazu Kozu, Sadamu Yamagata, Naoto Murao,
624 Sachio Ohta, Satoru Shiya, and Tatsuo Ohba. Effect of superficial ve-
625 locity on tar from downdraft gasification of biomass. *Energy & Fuels*,
626 19:1186–1191, 2005.
- 627 [46] S. Jarungthammachote and A. Dutta. Thermodynamic equilibrium
628 model and second law analysis of a downdraft waste gasifier. *Energy*,
629 32(9):1660 – 1669, 2007.
- 630 [47] Giulio Allesina, Simone Pedrazzi, Luca Guidetti, and Paolo Tartarini.
631 Modeling of coupling gasification and anaerobic digestion processes for
632 maize bioenergy conversion. *Biomass and Bioenergy*, 81:444 – 451, 2015.
- 633 [48] Giulio Allesina, Simone Pedrazzi, Federico Sgarbi, Elisa Pompeo,
634 Camilla Roberti, Vincenzo Cristiano, and Paolo Tartarini. Approaching
635 sustainable development through energy management, the case of fongo

- 636 tongo, cameroon. *International Journal of Energy and Environmental*
637 *Engineering*, 6(2):121–127, 2014.
- 638 [49] Giulio Allesina, Simone Pedrazzi, Emma La Cava, Michele Orlandi,
639 Miriam Hanuskova, Caludio Fontanesi, and Paolo Tartarini. Energy-
640 based assessment of optimal operating parameters for coupled biochar
641 and syngas production in stratified downdraft gasifiers. In *International*
642 *Heat Transfer Conference 15, Kyoto, Japan*, 2014.
- 643 [50] Giulio Allesina, Simone Pedrazzi, and Paolo Tartarini. Modeling and
644 investigation of the channeling phenomenon in downdraft stratified
645 gasifiers. *Bioresource Technology*, 146(0):704 – 712, 2013.
- 646 [51] Ranjani V. Siriwardan, Ming-Shing Shen, and Edward P. Fisher. Ad-
647 sorption of co2 on zeolites at moderate temperatures. *Energy and Fuels*,
648 19:1153–1159, 2005.
- 649 [52] Thana Phuphuakrat, Tomoaki Namioka, and Kunio Yoshikawa. Absorp-
650 tive removal of biomass tar using water and oily materials. *Bioresource*
651 *Technology*, 102(2):543–549, 2011.
- 652 [53] Shunsuke Nakamura, Shigeru Kitano, and Kunio Yoshikawa. Biomass
653 gasification process with the tar removal technologies utilizing bio-oil
654 scrubber and char bed. *Applied Energy*, 170:186 – 192, 2016.
- 655 [54] S. Pedrazzi, G. Zini, and P. Tartarini. Complete modeling and soft-
656 ware implementation of a virtual solar hydrogen hybrid system. *Energy*
657 *Conversion and Management*, 51(1):122 – 129, 2010.

- 658 [55] Simone Pedrazzi, Giulio Allesina, Alberto Muscio, and Paolo Tartarini.
659 Modeling and simulation of a dg-sofc-mgt hybrid system. In *7° Con-*
660 *gresso Nazionale AIGE, Rende (CZ) Italy*, 2013.
- 661 [56] Simone Pedrazzi. *Modeling and optimization of advanced systems for*
662 *electrical energy production from wood biomass*. PhD thesis, HIGH ME-
663 CHANICS AND AUTOMOTIVE DESIGN & TECHNOLOGY, Univer-
664 sity of Modena and Reggio Emilia, Dep. of Engineering 'Enzo Ferrari',
665 2013.
- 666 [57] DOE. *Fuel Cell Handbook (Seventh Edition)*. 2004.
- 667 [58] Zhiqi Wang, Tao He, Jianguang Qin, Jingli Wu, Jianqing Li, Zhongyue
668 Zi, Guangbo Liu, Jinhui Wu, and Li Sun. Gasification of biomass with
669 oxygen-enriched air in a pilot scale two-stage gasifier. *Fuel*, 150:386 –
670 393, 2015.
- 671 [59] H.A.M. Knoef. *Handbook of Biomass Gasification, Second Edition*.
672 BTG, 2012.
- 673 [60] Francesco Patuzzi, Dario Prando, Stergios Vakalis, Andrea Maria Rizzo,
674 David Chiaramonti, Werner Tirler, Tanja Mimmo, Andrea Gasparella,
675 and Marco Baratieri. Small-scale biomass gasification {CHP} systems:
676 Comparative performance assessment and monitoring experiences in
677 south tyrol (italy). *Energy*, 112:285 – 293, 2016.
- 678 [61] S. Pedrazzi, G. Allesina, and P. Tartarini. Aige conference: A kinetic
679 model for a stratified downdraft gasifier experimental assessment and

680 modeling of energy conversion effectiveness in a gasification power plant.
681 *International Journal of Heat and Technology*, 30(1):41–44, 2012.

682 **Figure captions and tables**

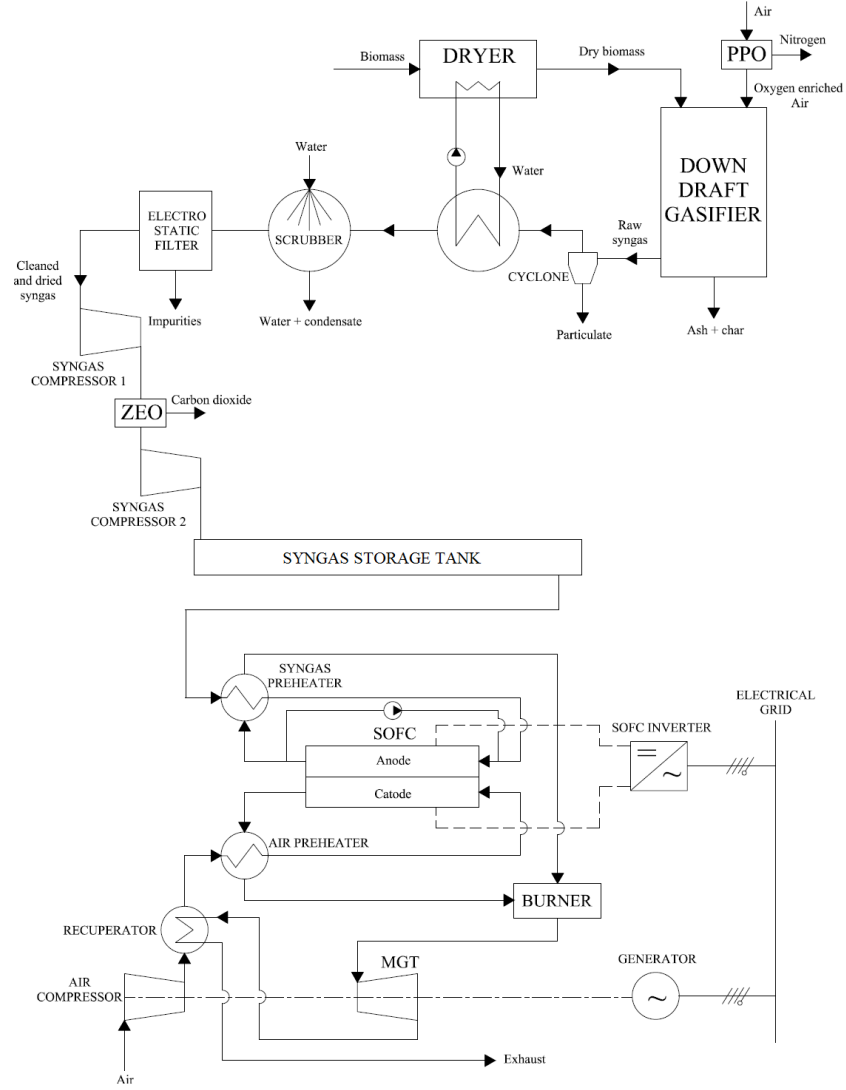


Figure 1: DG-SOFC-MGT hybrid system with zeolite CO_2 adsorption and oxygen-enriched air layout

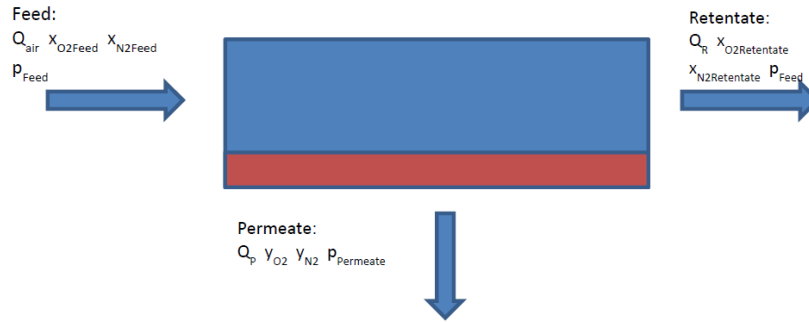


Figure 2: Oxygen enriched air membrane separator principle

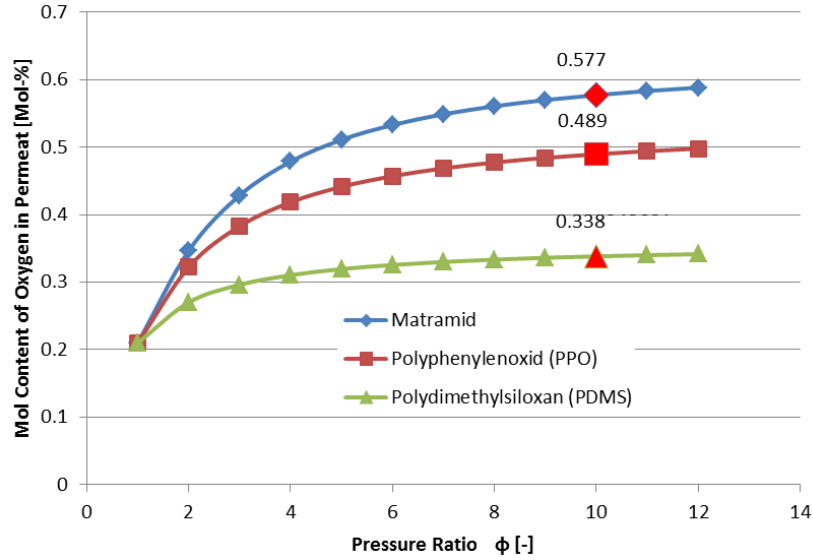


Figure 3: Characteristics of the separation membranes

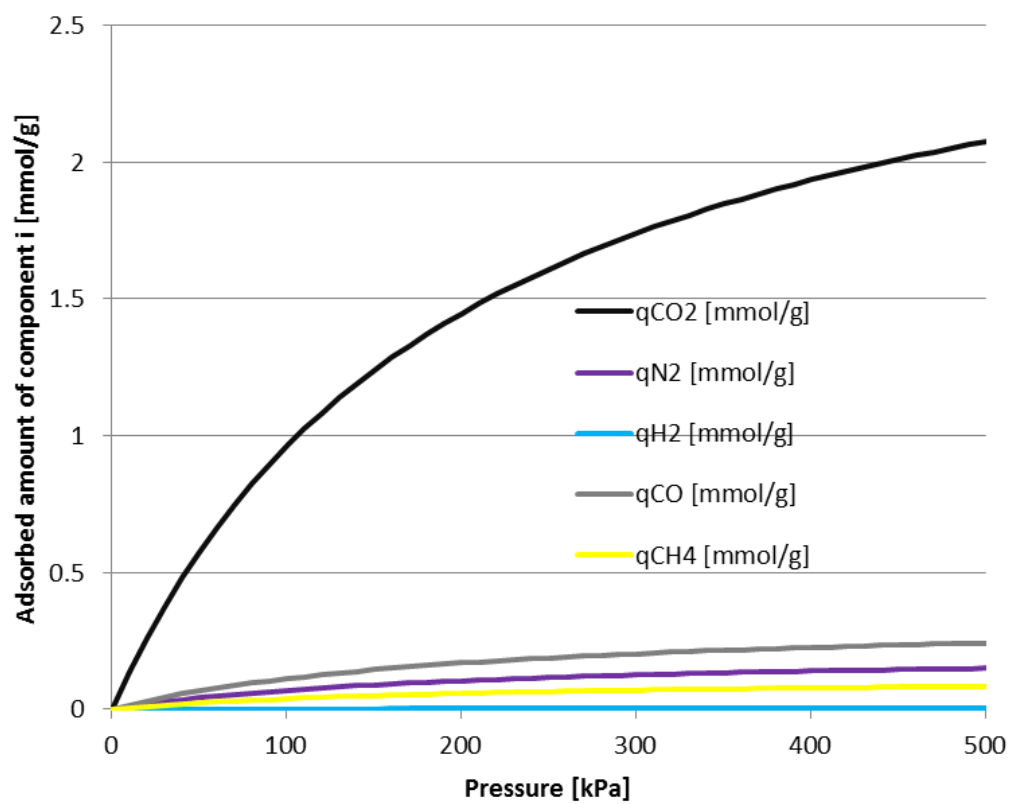


Figure 4: Zeolite 5A adsorbing curve Vs. pressure

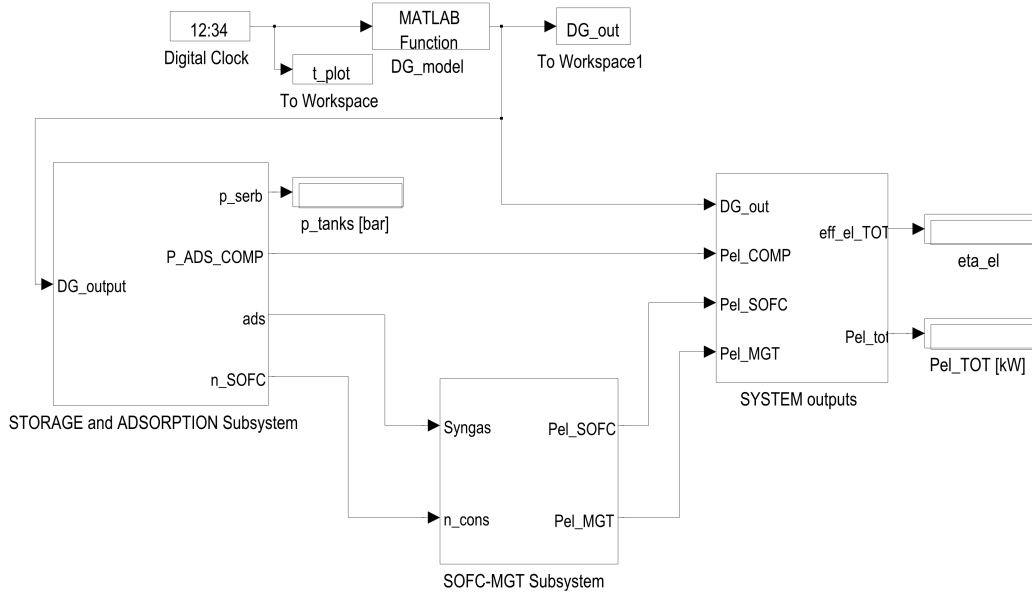


Figure 5: DG-SOFC-MGT hybrid system with zeolite CO_2 adsorption and oxygen-enriched air implemented in Matlab SimulinkTM

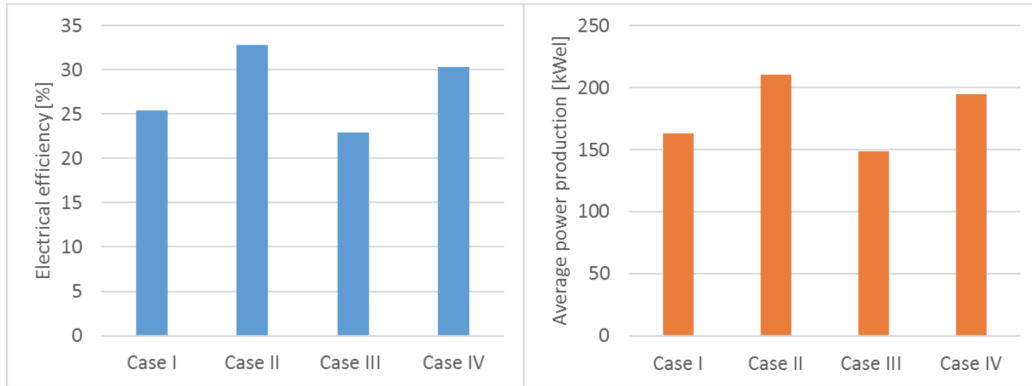


Figure 6: Efficiencies and electrical production values of the studied cases

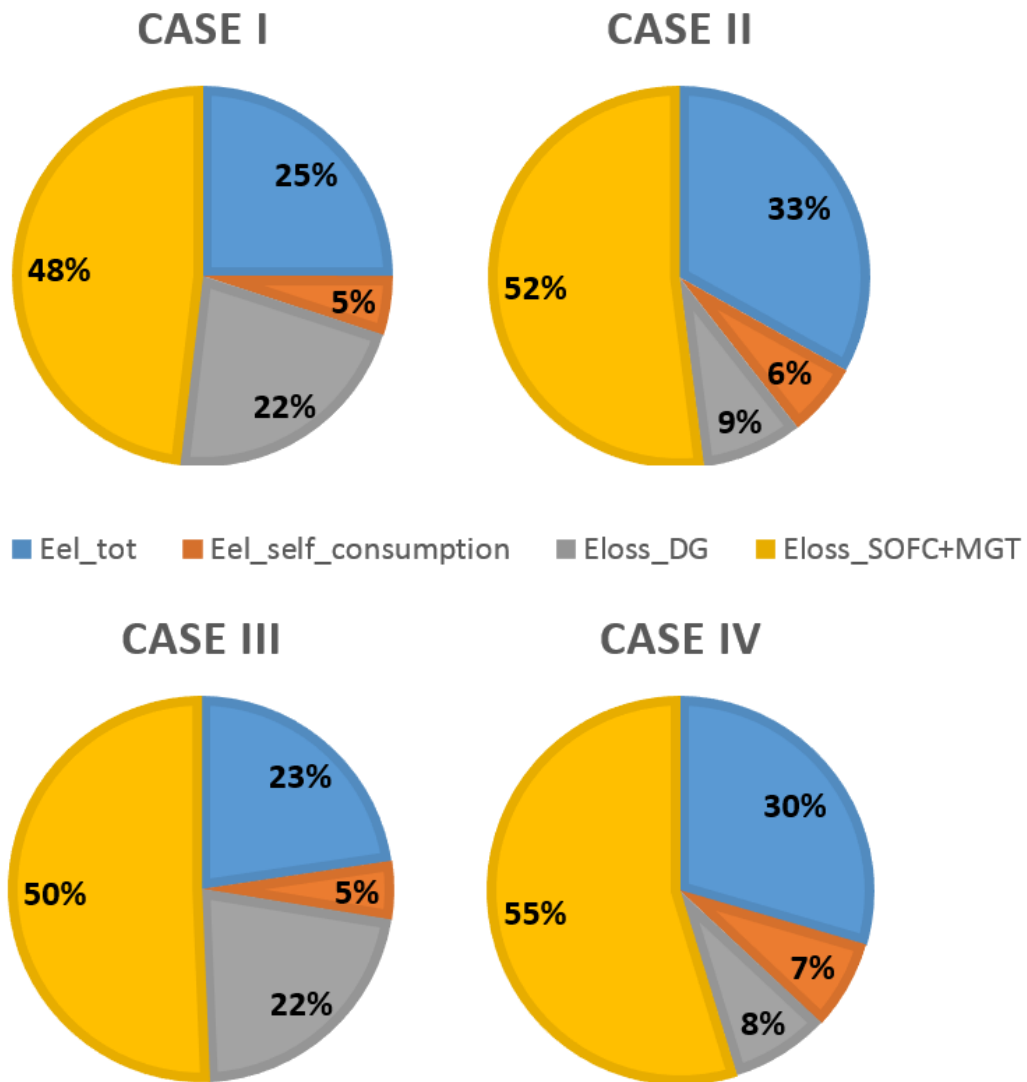


Figure 7: Energy balances of the studied cases

Table 1: Model parameters I

Membranes properties [31]		
Material	Selectivity α [ad]	Oxygen Permeability γ [mol m ⁻² s ⁻¹ bar ⁻¹]
Matrimid	6.7	62.0 x 10 ⁻⁵
PPO	4.7	37.2 x 10 ⁻⁴
PDMS	2.1	39.6 x 10 ⁻²
Poplar wood chips properties [61]		
Description	Symbol	Value
Total moisture	M	10 %
Carbon content (as received)	C_{ar}	41.62 %
Hydrogen content (as received)	H_{ar}	5.30 %
Nitrogen content (as received)	N_{ar}	0.52 %
Oxygen content (as received)	O_{ar}	39.81 %
Ash content	ASH	2.75 %
Higher heating value (dry basis)	HHV_{db}	15.7 MJ/kg
Gasifier model parameters[48]		
Description	Symbol	Value
As received biomass consumption	\dot{m}_{bio}	187 kg/h
Nominal gasifier thermal power	$P_{th,gas}$	800 kW
Initial calculation temperature	T_{in}	900 K
Pressure	p	1 atm
Equivalence ratio	ER	0.335
Gasifier and filters auxiliary consumption	$P_{DG,self}$	12.5 kW
Cyclic operation hours	$h_{operation}$	360 h
Cyclic maintenance hours	$h_{maintenance}$	4 h
Zeolite 5A parameters of adsorption at 303 K [39]		
Component	B [1/kPa]	q_m [mmol/g]
CO_2	0.019500	3.91900
H_2	0.000361	0.54464
N_2	0.000837	2.62543
CH_4	0.002535	2.75403
CO	0.004350	2.75800

Table 2: Model parameters II

Storage and compressor model parameters		
Description	Symbol	Value
Politropic exponent of the syngas [54]	m	1.33
Syngas compressor efficiency [54]	η_{comp}	92 %
Storage tank temperature	T_s	298.15 K
Initial syngas amount in the tanks	n_{in}	$7 * 10^4$ mol
Total tanks volume	V	650 m ³
SOFC model parameters		
Description	Symbol	Value
Fuel utilization factor	U_f	0.85
Recirculation factor	r	0.2
Operating temperature	T_{sofc}	1073.15 K
Anode pressure loss	Δp_a	500 Pa
Cathode pressure loss	Δp_c	1000 Pa
Anode pressure loss	Δp_a	500 Pa
Current density	i	300 mA/cm ²
Active cell area	A_{cell}	81 cm ²
Cells for each stack	$n_{cell,stack}$	75 cells
Number of stacks	n_{stack}	145 stacks
Cathode air excess	$vent$	1.15
Pressure ratio	PR	2.5
Steam to carbon coefficient	STC	1.4
Electrochemical parameters taken from [18]		
MGT model parameters [18]		
Description	Symbol	Value
Politropic exponenet of the air	m	1.33
Turbine isentropic efficiency	$\eta_{is,turb}$	84 %
Air compressor isentropic efficiency	$\eta_{is,comp}$	75 %
Turbine mechanical efficiency	$\eta_{mec,turb}$	99 %
Air compressor mechanical efficiency	$\eta_{mec,comp}$	98 %
Recuperator effectiveness	η_{rec}	85 %
Burner efficiency	$\eta_{eff,burner}$	99 %
MGT generator efficiency	$\eta_{alt,MGT}$	95 %
Pressure ratio	PR	2.5

Table 3: Case I (Gasifier + SOFC + MGT) simulation results

Gasifier		
Description	Symbol	Value
H_2 syngas fraction	x_{H_2}	19.03 %
H_2O syngas fraction	x_{H_2O}	7.78 %
CO syngas fraction	x_{CO}	15.10 %
CH_4 syngas fraction	x_{CH_4}	1.18 %
CO_2 syngas fraction	x_{CO_2}	13.99 %
N_2 syngas fraction	x_{N_2}	42.92 %
Air inlet flow	Q_{air}	2.94 mol/s
Syngas molar flow	\dot{n}_{syngas}	5.01 mol/s
Syngas higher heating value	$HHV_{syngas,db}$	4.75 MJ/Nm ³
Specific volumetric tar production	m_{tar,Nm^3}	23.63 g/Nm ³
Gasifier cold gas efficiency	η_{cold}	78.98 %
Average temperature of gasification	T	895 K
SOFC + MGT		
Description	Symbol	Value
Syngas molar flow to SOFC-MGT unit	\dot{n}_{SOFC}	4.95 mol/s
SOFC electrical power production	P_{SOFC}	136.70 kW
MGT electrical power production	P_{MGT}	60.73 kW
Total SOFC-MGT electrical power production	$P_{SOFC+MGT}$	197.43 kW
SOFC+MGT electrical efficiency	$\eta_{SOFC+MGT}$	37.46 %
Overall system		
Description	Symbol	Value
Storage tank pressure range	p_{serv}	2.67-5.39 bar
Average electrical auxiliary consumption	P_{self}	34.24 kW _{el}
Average electrical total power production	P_{tot}	163.19 kW _{el}
Average total electrical efficiency	η_{tot}	25.43 %

Table 4: Case II (PPO + Gasifier + SOFC + MGT) simulation results

PPO module		
Air inlet flow	Q_{air}	2.97 mol/s
Permeate molar flow	Q_P	1.27 mol/s
Retentate molar flow	Q_R	1.69 mol/s
Molar fraction of O_2 in permeate	y_{O_2}	48.9 %
Molar fraction of N_2 in permeate	y_{N_2}	51.1 %
Electric power consumption	$P_{el,PPO}$	15.3 kW
Gasifier		
Description	Symbol	Value
H_2 syngas fraction	x_{H_2}	28.49 %
H_2O syngas fraction	x_{H_2O}	9.91 %
CO syngas fraction	x_{CO}	26.33 %
CH_4 syngas fraction	x_{CH_4}	1.66 %
CO_2 syngas fraction	x_{CO_2}	17.2 %
N_2 syngas fraction	x_{N_2}	16.41 %
Syngas molar flow	\dot{n}_{syngas}	3.589 mol/s
Syngas higher heating value	$HHV_{syngas,db}$	7.55 MJ/Nm ³
Specific volumetric tar production	m_{tar,Nm^3}	0.27 g/Nm ³
Gasifier cold gas efficiency	η_{cold}	92.0 %
Average temperature of gasification	T	931 K
SOFC + MGT		
Description	Symbol	Value
Syngas molar flow to SOFC-MGT unit	\dot{n}_{SOFC}	3.545 mol/s
SOFC electrical power production	P_{SOFC}	184.20 kW
MGT electrical power production	P_{MGT}	68.33 kW
Total SOFC-MGT electrical power production	$P_{SOFC+MGT}$	252.53 kW
SOFC+MGT electrical efficiency	$\eta_{SOFC+MGT}$	42.08 %
Overall system		
Description	Symbol	Value
Storage tank pressure range	p_{serv}	2.67-4.62 bar
Average electrical auxiliary consumption	P_{self}	42.01 kW _{el}
Average electrical total power production	P_{tot}	210.52 kW _{el}
Average total electrical efficiency	η_{tot}	32.81 %

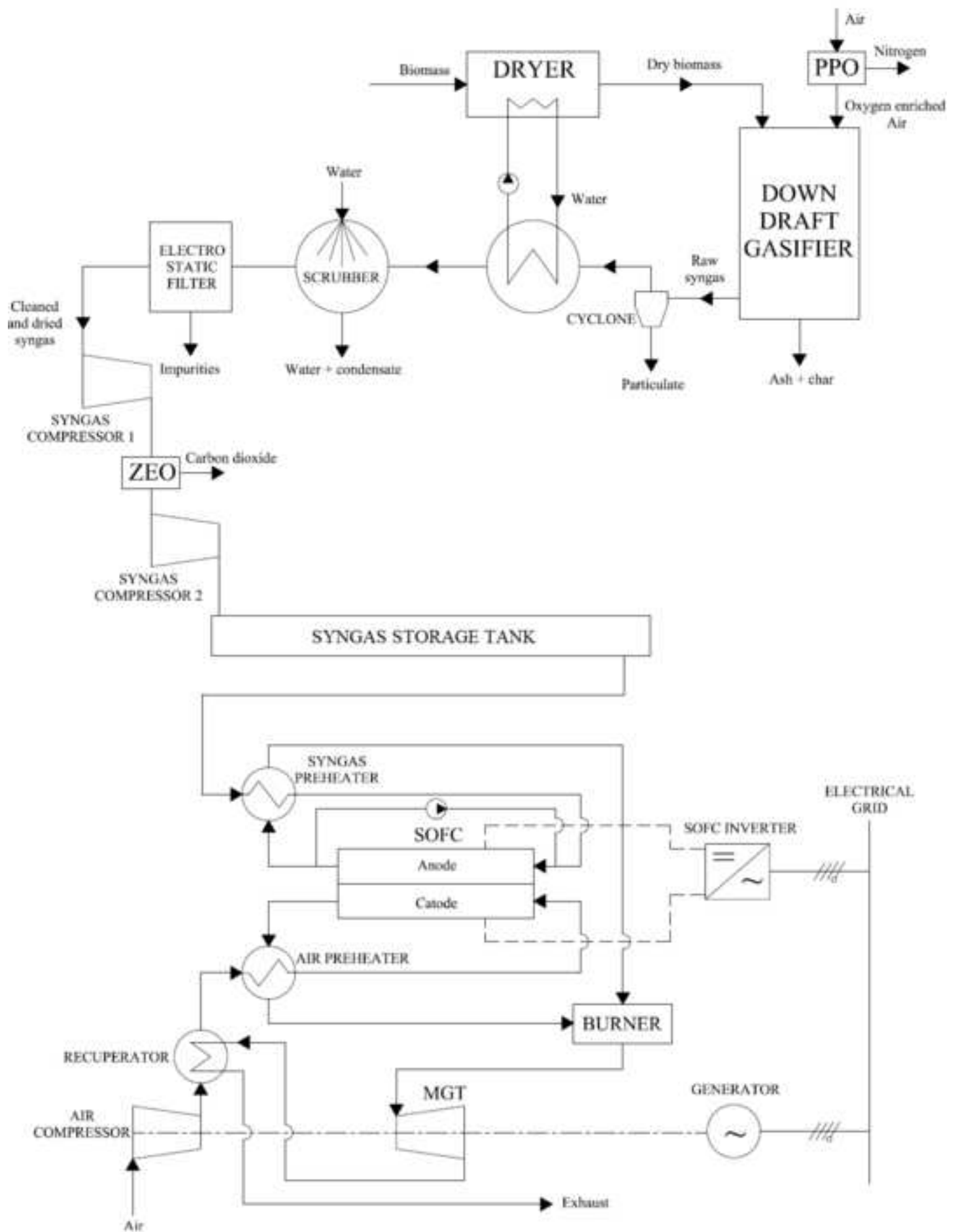
Table 5: Case III (Gasifier + ZEO + SOFC + MGT) simulation results

Gasifier (see Case I)		
ZEO		
Description	Symbol	Value
H_2 syngas fraction after adsorption	x_{H_2}	25.36 %
CO syngas fraction after adsorption	x_{CO}	17.08 %
CH_4 syngas fraction after adsorption	x_{CH_4}	1.43 %
CO_2 syngas fraction after adsorption	x_{CO_2}	0.39 %
N_2 syngas fraction after adsorption	x_{N_2}	55.73 %
Syngas molar flow after adsorption	\dot{n}_{syngas}	4.065 mol/s
Syngas higher heating value after adsorption	$HHV_{syngas,db}$	5.9 MJ/Nm ³
Active zeolite mass for every regeneration cycle	$m_{z eo}$	23.742 kg
SOFC + MGT		
Description	Symbol	Value
Syngas molar flow to SOFC-MGT unit	\dot{n}_{SOFC}	4.020 mol/s
SOFC electrical power production	P_{SOFC}	138.50 kW
MGT electrical power production	P_{MGT}	44.00 kW
Total SOFC-MGT electrical power production	$P_{SOFC+MGT}$	182.5 kW
SOFC+MGT electrical efficiency	$\eta_{SOFC+MGT}$	34.33 %
Overall system		
Description	Symbol	Value
Storage tank pressure range	p_{serb}	2.66-4.88 bar
Average electrical auxiliary consumption	P_{self}	33.76 kW _{el}
Average electrical total power production	P_{tot}	148.74 kW _{el}
Average total electrical efficiency	η_{tot}	22.87 %

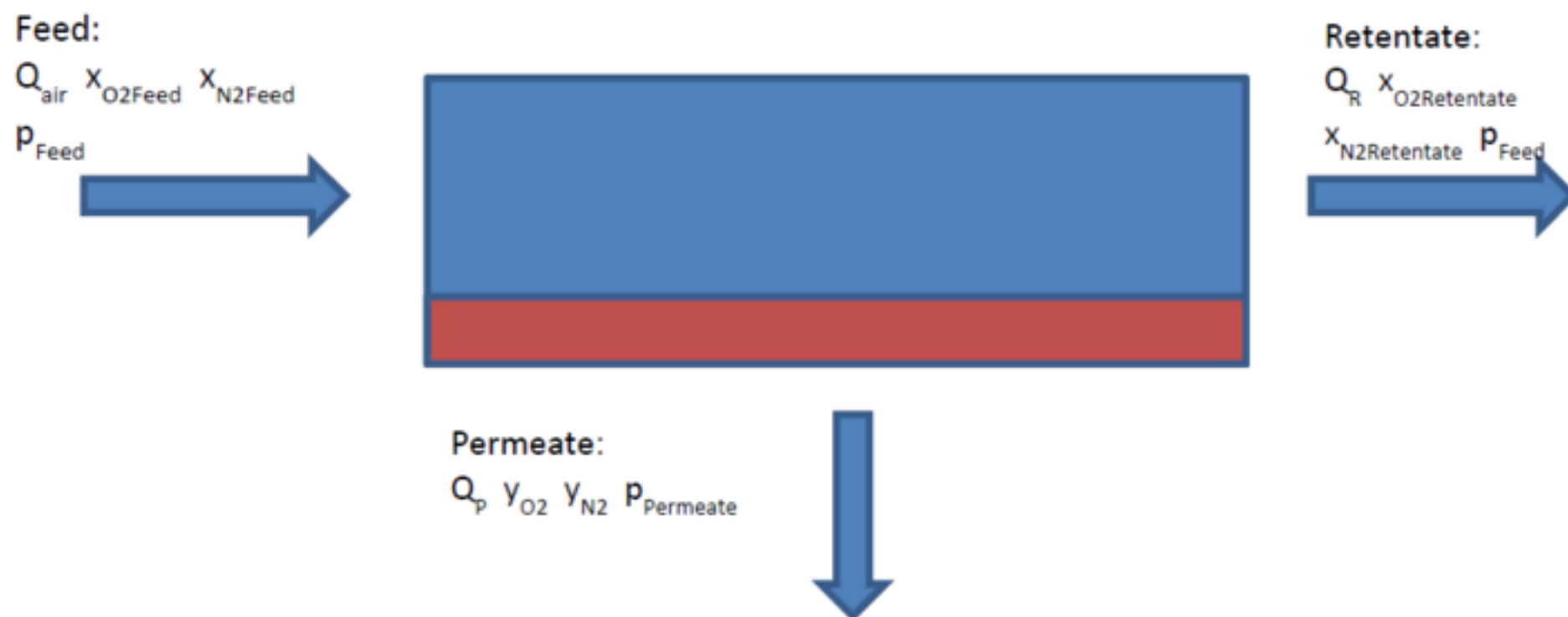
Table 6: Case IV (PPO + Gasifier + ZEO + SOFC + MGT) simulation results

PPO module (see Case II)		
Gasifier (see Case II)		
ZEO		
Description	Symbol	Value
H_2 syngas fraction after adsorption	x_{H_2}	41.53 %
CO syngas fraction after adsorption	x_{CO}	32.54 %
CH_4 syngas fraction after adsorption	x_{CH_4}	2.21 %
CO_2 syngas fraction after adsorption	x_{CO_2}	0.43 %
N_2 syngas fraction after adsorption	x_{N_2}	23.30 %
Syngas molar flow after adsorption	\dot{n}_{syngas}	2.726 mol/s
Syngas higher heating value after adsorption	$HHV_{syngas,db}$	10.19 MJ/Nm ³
Active zeolite mass for every regeneration cycle	m_{zeo}	20.244 kg
SOFC + MGT		
Description	Symbol	Value
Syngas molar flow to SOFC-MGT unit	\dot{n}_{SOFC}	2.696 mol/s
SOFC electrical power production	P_{SOFC}	184.70 kW
MGT electrical power production	P_{MGT}	51.80 kW
Total SOFC-MGT electrical power production	$P_{SOFC+MGT}$	236.50 kW
SOFC+MGT electrical efficiency	$\eta_{SOFC+MGT}$	38.41 %
Overall system		
Description	Symbol	Value
Storage tank pressure range	p_{serb}	2.66-4.15 bar
Average electrical auxiliary consumption	P_{self}	51.80 kW _{el}
Average electrical total power production	P_{tot}	194.53 kW _{el}
Average total electrical efficiency	η_{tot}	30.32 %

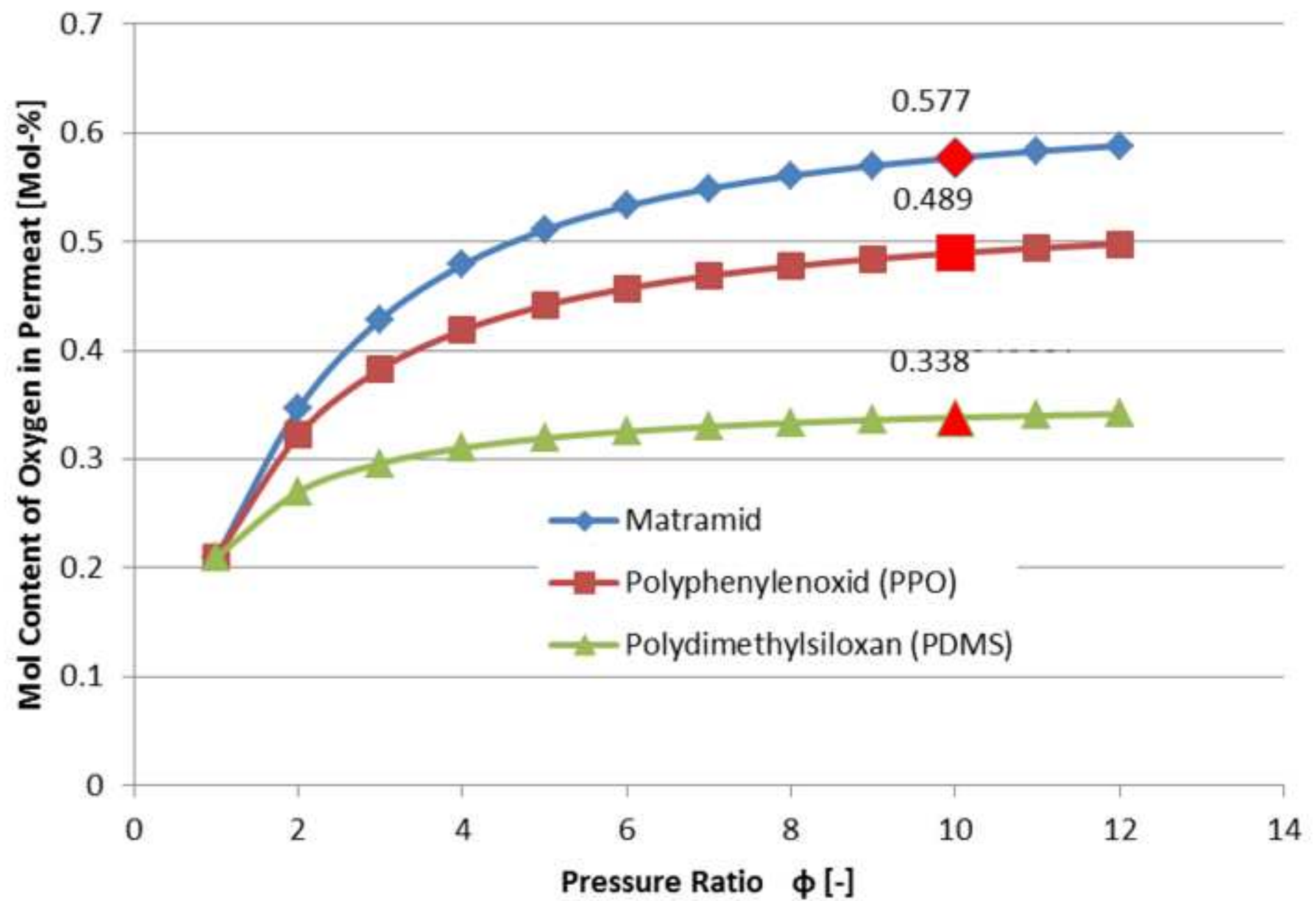
Figure(s)
[Click here to download high resolution image](#)



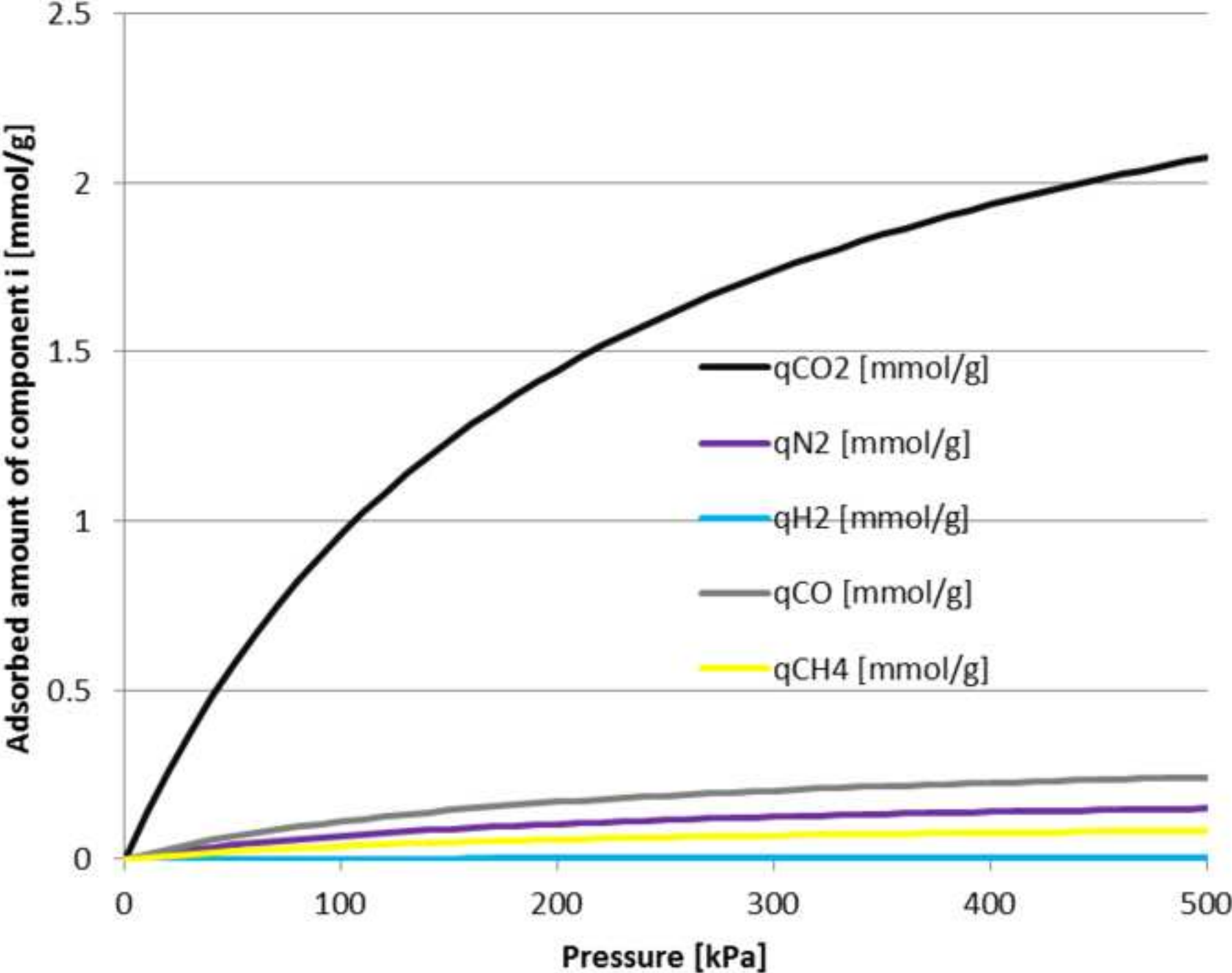
Figure(s)
[Click here to download high resolution image](#)



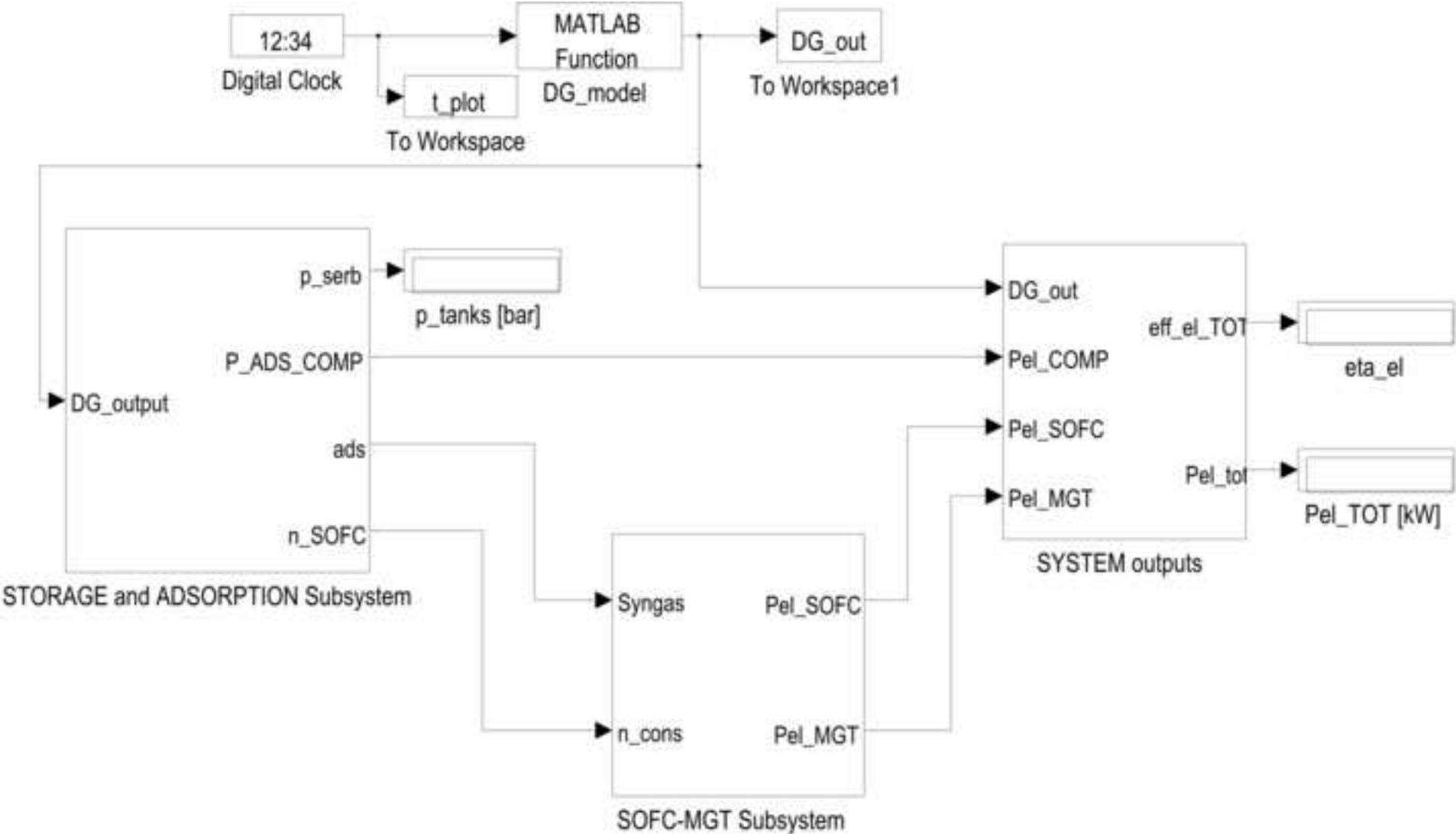
Figure(s)
[Click here to download high resolution image](#)



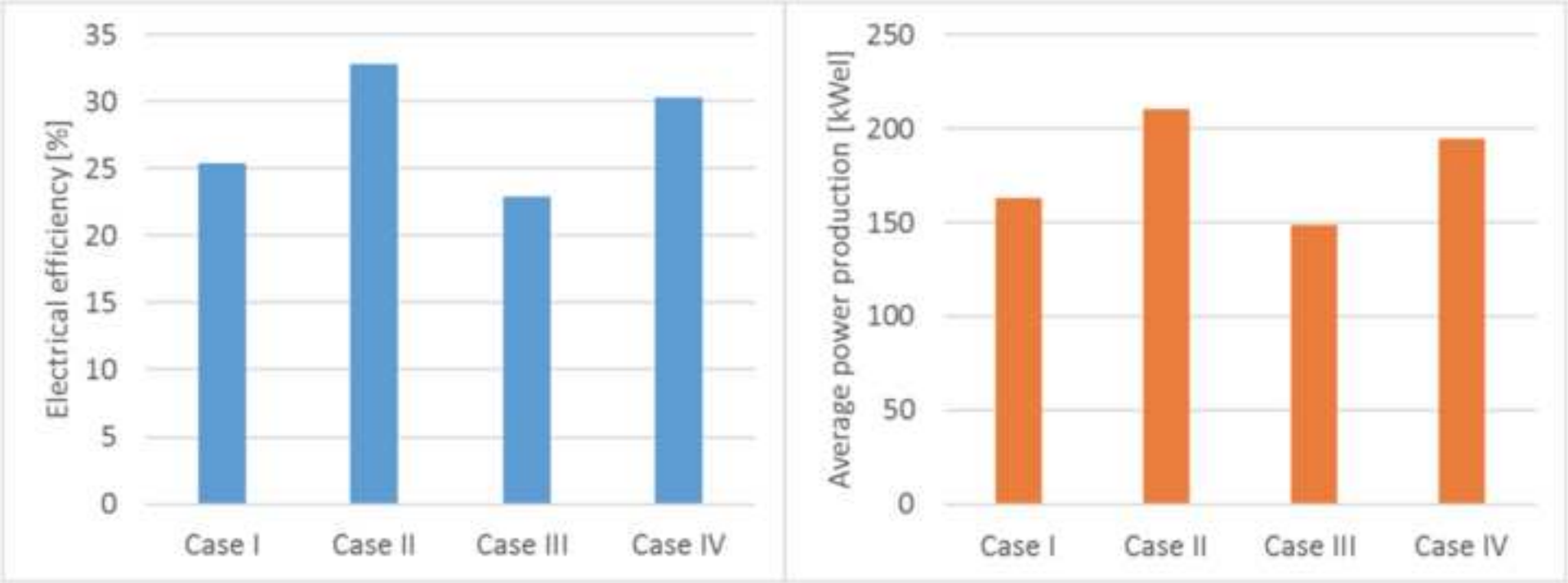
Figure(s)
[Click here to download high resolution image](#)

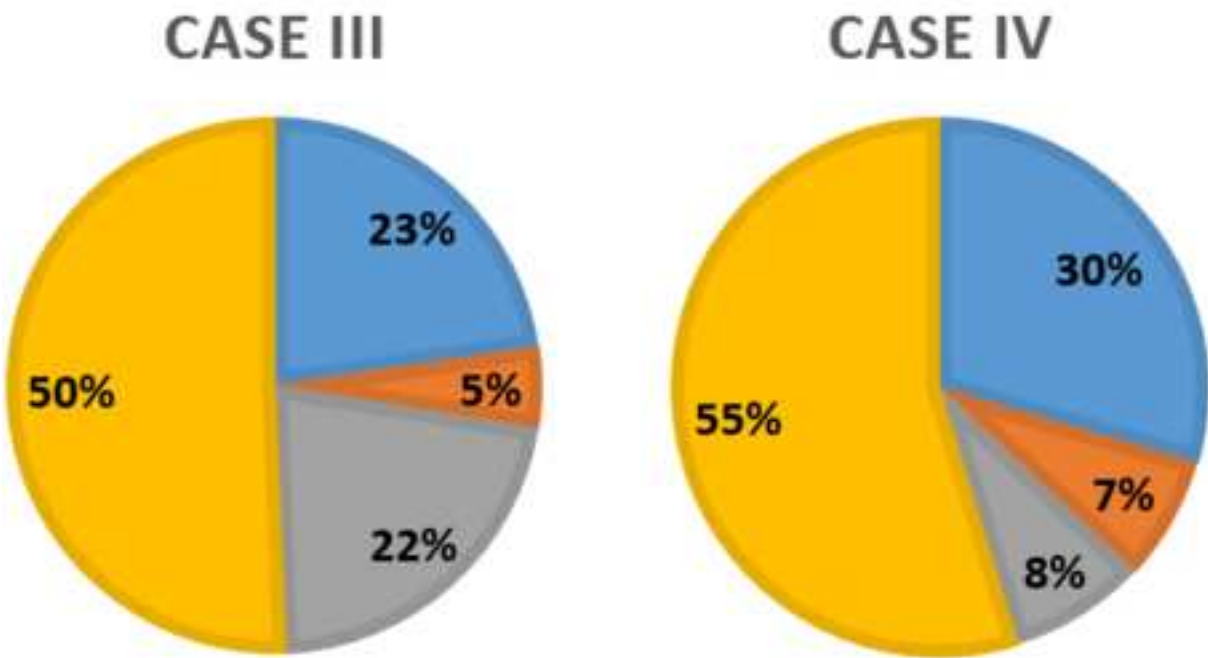
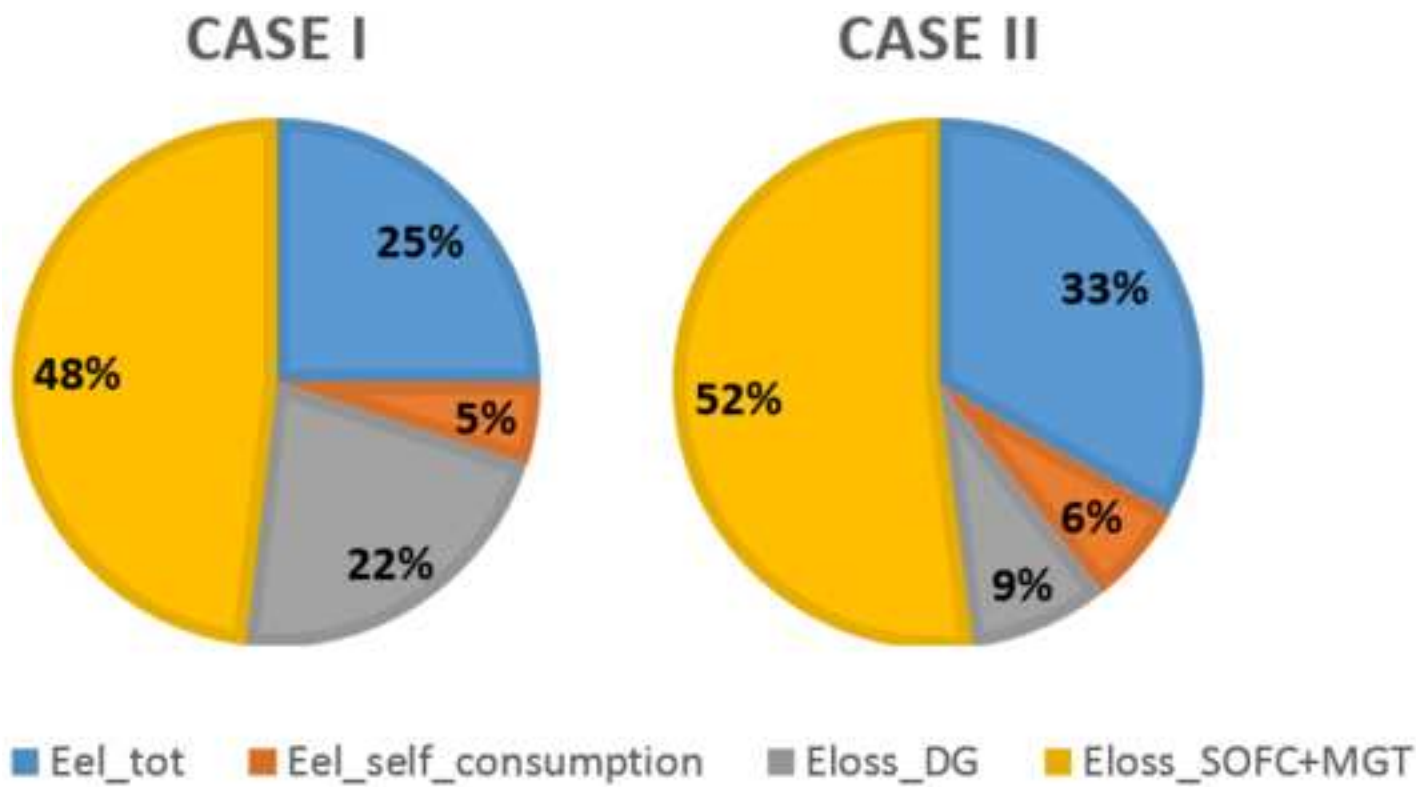


Figure(s)
[Click here to download high resolution image](#)



Figure(s)
[Click here to download high resolution image](#)





Response to Review Comments

Thanks to the reviewers for their work, I have revised my present research paper in the light of their useful suggestions and comments. The corrections in the manuscript were made in red color. I hope my revision has improved the paper to the level of their satisfaction:

(O) = reviewer observation

(A) = author answer

Editor

(O): Please update your literature survey by referring to the most recent and relevant references that have been published in highly ranked and prestigious journals including this journal. Please focus on relevant publications during the last few years.

(A): We add 5 recent references about fuel cells systems in the introduction section

Reviewer # 1

(O): The manuscript should be carefully checked again for typos, for example: line 18, 43, and 415 etc..

(A): Done

(O): A nomenclature section is needed to quickly refer to any symbol/acronym during the reading of the article.

(A): Done

(O): Fig. 5, Simulink model is not properly visible. An increase in font size or style maybe required.

(A): Done

(O): In introduction section, the authors have emphasized largely on the importance of PPO or ZEO module and their working principle. In one way, this is important to explain all details. But the reviewer suggest that trivial details about importance of PPO or ZEO module should be mentioned briefly with proper literature references (for further study) and more focus should be on literature review of these modules and their effect on the efficiency of the system. I could not find the authors mentioning any study related to this scope of work.

(A): Several works about PPO membrane air filtration and zeolites adsorption applications are now cited in the introduction section.

(O): The conclusion section maintains that including the PPO and ZEO might result in higher efficiencies, which is major focus of this paper. But, in results section, the discussion related to comparison of these cases with existing energy conversion systems (IC engine or ORC etc.) might be missing/less emphasized. It is suggested that a detailed comparison of energy conversion efficiencies of other technologies may be included in the discussion section.

(A): We add a comparison with a common gasifier-IC engine power plant in the “Performance and energy consideration” subsection.

(O): Table 1 (page 38), gasifier model parameters reference for data may be furnished.

(A): Reference added

(O): Table 3-6 show data obtained from different cases during simulation. It is suggested that a brief summary of all simulation results (in the form of a graph) might be helpful for the reader to get an overview of the results.

(A): Figure 6 reports efficiency and power production results reported in Table 3-6. In addition Figure 7 shows energy results of the fourth cases.

Thank you again for your review.

All the best,

Simone Pedrazzi

Effects of upgrading systems on energy conversion efficiency of a gasifier - fuel cell - gas turbine power plant

Simone Pedrazzi^{a,*}, Giulio Allesina^a, Paolo Tartarini^a

^a*University of Modena and Reggio Emilia, Department of Engineering 'Enzo Ferrari',
Via Vivarelli 10/1, 41125 Modena, Italy*

Abstract

THIS PAPER IS SUBMITTED WITH THE OPTION 'YOUR PAPER YOUR WAY'. FOR THIS REASON LAYOUT AND STYLE MAY DIFFER FROM THE JOURNAL ONE.

This work focuses on a DG-SOFC-MGT (downdraft gasifier- solid oxide fuel cell - micro gas turbine) power plant for electrical energy production and investigates two possible performance-upgrading systems: polyphenylene oxide (PPO) membrane and zeolite filters. The first is used to produce oxygen-enriched air **used in** the reactor, while the latter separates the CO_2 content from the syngas. In order to prevent power plant shutdowns during the gasifier reactor scheduled maintenance, the system is equipped with a gas storage tank. The generation unit consists of a SOFC-MGT system characterized by higher electrical efficiency when compared to conventional power production technology (IC engines, ORC and EFGT). Poplar wood chips with 10% of total moisture are used as feedstock. Four different combinations with and without PPO and zeolite filtrations are simulated and discussed. One-year

*Corresponding author

Email address: simone.pedrazzi@unimore.it (Simone Pedrazzi)

energy and power simulation were used as basis for comparison between all the cases analyzed. The modeling of the gasification reactions gives results consistent with literature about oxygen-enriched processes. Results showed that the highest electrical efficiency obtained is 32.81%. This value is reached by the power plant equipped only with PPO membrane filtration. Contrary to the PPO filtering, zeolite filtration does not increase the SOFC-MGT unit performance while it affects the energy balance with high auxiliary electrical consumption. This solution can be considered valuable only for future work coupling a CO_2 sequestration system to the power plant.

Keywords:

Biomass, Gasification, Modeling, Solide Oxide Fuel Cells, Zeolites, PPO membrane

1. Introduction

Due to the abundant availability and distribution, biomasses hold key-roles in plans for renewable energy production. This trend is becoming even more relevant thanks to the good degree of reliability and efficiency of the biomass-based technologies together with the high subsidies granted by several government for sustainable electrical energy production [1].

Depending on the feedstock quality and availability, biomasses are converted into energy through different technologies. In the case of ligno-cellulosic biomasses, a technology of great validity is gasification. This thermo-chemical process turns solid biomass into a gaseous fuel known as syngas, which can be converted into electrical energy through all those systems used for power production from gaseous fuels [2]. Gasification is today one of the most effi-

cient technologies to convert wood into electricity and it is also sustainable in terms of the environmental balance of CO_2 [3, 4].

Most of the gasification power plants use an IC engine-generator to convert the syngas chemical energy into electrical power. However, in some cases other conversion machines are used, i.e. Organic Rankine Cycles (ORC), External Firing Gas Turbines (EFGT)[5] and Stirling engines are used with the major advantage of having minor limitation about the syngas level of purification [2, 6, 7, 8, 9]. These systems are usually characterized by low conversion efficiencies of about 10-12%. Major conversion rates can be obtained only with electrochemical devices such as proton exchange membrane fuel cells [10], Molten Carbonate Fuel Cells (MCFC) [11, 12], Solid Oxide Fuel Cells (SOFC) [13, 14, 15], systems composed of SOFC and Micro Gas Turbines (MGT) [16, 17, 18, 19, 20, 21, 22, 23, 24, 25, 26] and systems composed of SOFC-MGT-ORC [27]. Despite the high rate of energy conversion, these systems require perfectly clean syngas [28]. Downdraft gasifiers are the most suitable architecture due to the low tar and particulate content in their gas when compared to updraft, crossdraft or fluidized bed gasifiers [2, 6, 29]. However, downdraft gasifiers commonly use air as gasification agent. This solution generates a syngas with a low calorific value where the hydrogen, methane and carbon monoxide are diluted in non-burnable gases: N_2 (about 50%) and CO_2 (from 10 to 20%). Otherwise, it is possible to choose oxygen gasification that produces a syngas with negligible N_2 content. However, oxygen gasification is a complex and expensive technology due to the gasification agent supply sub-systems and reactor material choice. Indeed, temperatures inside the reactor can reach 1200-1300 K when oxygen is used instead of air

38 [30].

39 The basic system discussed in this study is composed of an air blown-
40 downdraft-fixed bed gasifier fed with poplar wood chips. This work is aimed
41 at investigating the effects of different power plant designs on the overall
42 energy conversion efficiency.

43 The first power plant upgrading sub-system consists of a polyphenylene
44 oxide (PPO) membrane used to produce oxygen-enriched air. The gas sep-
45 aration characterization of this membrane is reported in literature [31, 32].
46 In practice, membrane gas separation is applied to increase the oxygen con-
47 tent in the inlet air of biomass boilers [33]. Bisio et al. studied the ther-
48 modynamics of combustion with enriched air and reviewed several types of
49 membranes [34]. Coombe and Nieh developed a membrane-based device for
50 air enrichment in small scale burners [35]. Hao et al. applied an oxygen-
51 permeable membrane to a reactor for the co-production of dimethyl ether
52 (DME)/methanol and electricity [36]. This paper uses PPO membrane in
53 order to obtain air with about 50% of oxygen then used as gasification agent.
54 This solution is a hybrid between air and pure oxygen gasification. Enriched
55 air reduces the reactor thermal stress compared to pure oxygen gasification,
56 while the syngas has a lower N_2 content than the one obtained in pure air
57 gasification. In addition, the syngas flow rate decreases because, for a fixed
58 power output, the enriched air flow required for gasification is lower than air
59 used in conventional gasification. This happens because the same amount of
60 oxygen is used in both cases and its concentration in enriched air is higher
61 than untreated air. Finally, the tar production is lower than air gasification
62 as consequence of the higher temperature that cracks more efficiently the

63 primary tars from pyrolysis [37].

64 A second solution discussed in this work consists of a porous media used
65 to upgrade the syngas. In fact, syngas has a variable CO_2 content depending
66 on gasification process as well as several boundary conditions. This value
67 ranges from 10% to 30% and it reduces significantly the higher heating value
68 of the syngas [37]. A solution to overcome this issue is to adopt a pressure-
69 swing selective synthetic zeolite filter. This system is placed before the gas
70 storage in order to separate carbon dioxide from syngas [38, 39]. The filter
71 can be constantly regenerated using a rotary valve packaged into modules
72 as described by Tagliabue et al. [40]. Literature investigation about zeolite
73 filtration outlines several works. Bacsik et al. studied the biogas CO_2-CH_4
74 separation through zeolites [41]. Kacem et al. investigated the pressure swing
75 adsorption for CO_2/N_2 and CO_2/CH_4 separation using activated carbon and
76 several types of zeolites [42]. Dirar et al. investigated intrinsic adsorption
77 properties of CO_2 on 5A and 13X zeolite [43].

78 The syngas obtained from gasification is stored and then used in a SOFC
79 unit able to produce electrical and thermal energy. The number of stacks
80 within the cell is optimized taking into account the optimal electrical cur-
81 rent density. The chosen number guarantees a good efficiency, however the
82 gas discharged from the cell still contains some chemical energy. For this
83 reason, this work suggests to convert this residual energy in a micro gas tur-
84 bine (MGT). The syngas storage allows the generation unit to operate in its
85 optimal point, furthermore it prevent the power plant shouting down dur-
86 ing the maintenance operations of the gasifier. This management preserves
87 the SOFC and MGT reliability. However, it is difficult to design the stor-

age capacity because an oversize storage rises the systems costs, while an undersized capacity reduces the time gained for the maintenance. For this reason, the storage was designed taking into account the tanks pressure, the electrical power production of the SOFC-MGT unit and the time required for scheduled stops of the gasifier for maintenance operations.

The mathematics of the whole system was developed starting from literature. The overall model has been implemented in Matlab SimulinkTM software environment in order to simulate the behavior of the system under different conditions over a year long simulation.

2. System modeling

The basic system layout is reported in Figure 1. The most relevant components are:

- **Downdraft gasifier:** The gasifier is equipped with a subsystem for the syngas filtering and cooling with water scrubber and electrostatic filters.
- **Syngas storage:** It consists of a tank of a total volume of 650 m³.
- **SOFC unit:** This subsystem consists of 10875 solid oxide cells and it is connected to the electrical grid by a power inverter.
- **Micro gas turbine (MGT):** this turbo-machinery is used to convert the last part of chemical energy content in the syngas purged by the SOFC.

109 This work investigates the effect of the implementation of the following
110 sub-systems to the basic scheme:

111 • **PPO membrane filter module:** The PPO sub-system consists of
112 the membrane filter and a compressor that increases the pressure of
113 the air before the PPO membrane filter to about 1 MPa. The oxygen
114 enriched air is sent to the gasifier at atmospheric pressure. A flow of
115 nitrogen is purged from the PPO module.

116 • **Zeolite (ZEO) filter module:** the zeolite (ZEO) filter module is
117 placed after the first syngas compressor. There is a further syngas
118 compression stage ahead the storage tanks because the ZEO module
119 works at 0.5 MPa of pressure as described in Section 2.3, while the
120 pressure in the storage is often higher.

121 The syngas is used as fuel in the SOFC stack. In this device, the fuel
122 reforming occurs at the anode and there is a recirculation of the 20% of
123 the anode exhaust to increase the fuel reforming performance [18, 22]. The
124 anode exhaust is used to preheat the syngas, then it is finally burned in the
125 MGT burner together with the cathode exhaust. The air required for the
126 electrochemical reaction is compressed and preheated in the recuperator of
127 the MGT as well as in the air preheater of the SOFC.

128 The SOFC stack generates DC current which is converted into AC current
129 by an inverter and it is sent to the electrical grid. The MGT drags the air
130 compressor and the remaining mechanical energy is converted into electrical
131 energy by an alternator.

132 2.1. PPO module modeling

133 Polymeric membranes allow to separate different gaseous components de-
 134 pending on the pore size and pressure applied to the filter [31]. In this work
 135 a membrane is used to separate nitrogen from air. The membranes widely
 136 used for this purpose are: Matrimid, Polyphenylenoxide (PPO) and Poly-
 137 dimethylsiloxan (PDMS) [31]. As showed in Figure 2, in membranes the
 138 inlet air flow is divided in permeate and retentate molar flows. The inlet
 139 flow (Q_{air} [mol/s]) has a pressure p_{feed} [atm] and it is composed of x_{O_2Feed}
 140 and x_{N_2Feed} molar fractions of oxygen and nitrogen. The permeate molar
 141 flow (Q_P [mol/s]) has a pressure $p_{permeate}$ [atm] and it is composed of y_{O_2}
 142 and y_{N_2} molar fractions of oxygen and nitrogen. The retentate molar flow
 143 (Q_R [mol/s]) has a pressure p_{feed} [atm] and it is composed of $x_{O_2Retentate}$ and
 144 $x_{N_2Retentate}$ molar fractions of oxygen and nitrogen.

145 Each membrane behavior is identified through two parameters: the selec-
 146 tivity (α) and the permeability to oxygen (γ). The first factor represents the
 147 attitude of the membrane to attract oxygen, the second quantifies the atti-
 148 tude of the membrane to be crossed by it. High selectivity and permeability
 149 ensure great filtering performance in terms of high value of y_{O_2} and a small
 150 membrane surface area is required to filter a given amount of air. Table 1
 151 presents the parameters of Matrimid, PPO and PDSM membranes.

152 The choice of a PPO membrane is a compromise in terms of acceptable
 153 values of selectivity and permeability. In order to simulate the behavior of
 154 the membranes, a mathematical model has been implemented from Melin
 155 and Rautenbach [31]. The model is based on the following assumptions:

- 156 • Air is considered a binary gas mixture with 21% oxygen and 79% ni-

157 trogen.

- 158 • Steady state conditions.
- 159 • Isotherm conditions.
- 160 • Isobaric conditions.
- 161 • Perfect gas law.
- 162 • Constant permeability.
- 163 • Perfect mixing conditions on upstream and downstream sides.
- 164 • Concentration polarization at the membrane is neglected.
- 165 • Pressure loss in the porous support layer is neglected.
- 166 • The permeate can drain off freely.

167 The calculation of the permeate composition is made with the following
168 formula taken from the work of Melin and Rautenbach [31]:

$$y_{O_2} = \frac{1}{2} \left[1 + \phi * \left(x_{O_2 Feed} + \frac{1}{\alpha - 1} \right) \right] - \sqrt{\left[\frac{1}{2} \left[1 + \phi * \left(x_{O_2 Feed} + \frac{1}{\alpha - 1} \right) \right] \right]^2 - \frac{\alpha * \phi * x_{O_2 Feed}}{\alpha - 1}} \quad (1)$$

$$y_{N_2} = 1 - y_{O_2} \quad (2)$$

169 where ϕ [-] is the feed-permeate pressure ratio given by the following
170 equation:

$$\phi = p_{feed}/p_{permeate} \quad (3)$$

Figure 3 reports the permeate composition over pressure ratio for the three membrane types considered. It can be seen that only a certain maximum of oxygen ratio can be achieved because all the graphs are leveling off. Therefore a pressure ratio of 1 MPa was chosen for further calculations as suggested in Melin and Rautenbach [31] and the $p_{retentate}$ was fixed at 1 atm.

The Matrimid membrane is able to produce the highest oxygen ratio of 0.58 % vol. in the permeate, however PPO membrane presents a good value of oxygen ratio (0.49 % vol.) and an acceptable value of permeability, therefore this membrane is adopted in the simulations. The active area of the membrane can be assessed from the molar flow of oxygen required for the gasification Q_{PO_2} [mol/s]:

$$A_{membrane} = \frac{Q_{PO_2}}{\gamma * (x_{O_2Feed} * p_{feed} + y_{O_2} * p_{permeate})} \quad (4)$$

The molar flow of nitrogen Q_{PN_2} [mol/s] and the total permeate molar flow Q_P [mol/s] is given by the following equations:

$$Q_{PN_2} = \frac{\gamma}{\alpha} * [p_{feed} * (1 - x_{O_2Feed}) + p_{permeate} * (1 - y_{O_2})] \quad (5)$$

$$Q_P = Q_{PN_2} + Q_{PO_2} \quad (6)$$

The molar flow of the inlet air Q_{air} , the retentate molar flow Q_R and the retentate composition ($x_{O_2Retentate}$ and $x_{N_2Retentate}$) are calculated setting to zero the amount of oxygen in the retentate flow as suggested by Melin and

187 Rautenbach[31]. Thus, a mass balance equation can be applied to estimate
 188 Q_{air} and Q_R :

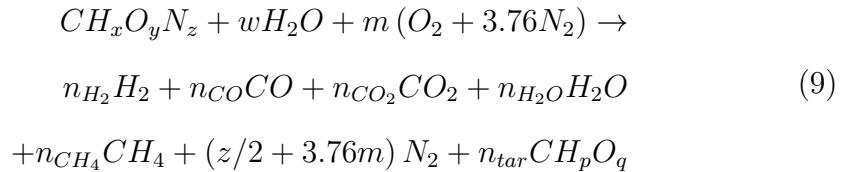
$$Q_{air} * x_{O_2 Feed} = Q_P * y_{O_2} \rightarrow Q_{air} = \frac{Q_P * y_{O_2}}{x_{O_2 Feed}} \quad (7)$$

$$Q_{air} = Q_P + Q_R \rightarrow Q_R = Q_{air} - Q_P \quad (8)$$

189 Finally, the electrical power consumption to pressurize the inlet air flow
 190 is calculated as a polytropic compression by Equation 15 assuming $T_{in} = 20$
 191 $^{\circ}C$; $m = 1.2$ and $\eta_{comp} = 90\%$.

192 2.2. Gasifier modeling

193 In this work, the gasification process is simulated using a black-box model
 194 based on Barman's work [44]. The model is validated for downdraft gasifiers;
 195 it is based on the following gasification equation:



196 where $CH_xO_yN_z$ is the equivalent chemical formula of "dry and ash
 197 free" (daf) biomass; CH_pO_q is the equivalent chemical formula of tar [45];
 198 $w [mol/mol_{bio}]$ is the specific molar amount of the biomass moisture; m
 199 $[mol/mol_{bio}]$ is the specific molar amount of oxygen calculated starting from
 200 the equivalence ratio ER as suggested by Jarungthammachote and Dutta[46];
 201 $n_{H_2}, n_{CO}, n_{CO_2}, n_{H_2O}, n_{CH_4}, n_{tar} [mol/mol_{bio}]$ are the specific molar amounts
 202 of $H_2, CO, CO_2, H_2O, CH_4$ and tar which constitute the syngas.

203 This model is used and discussed in several other works [47, 48, 49]. It
 204 consists of a chemical and a thermal sub-models that converge to the final
 205 composition of the gas. The first step is to choose an initial temperature T
 206 [K] and calculate the equilibrium constant of the following reactions:

- 207 • **K1:** Water-gas shift $CO + H_2O \leftrightarrow CO_2 + H_2$
- 208 • **K2:** Hydrogasification $C + 2H_2 \leftrightarrow CH_4$
- 209 • **K3:** Methane steam reforming $CH_4 + H_2O \leftrightarrow CO + 3H_2$

210 The system of equations 10 reported below is composed of three chemical
 211 balances calculated from Equation 9 (carbon, hydrogen and oxygen) and
 212 the three equilibrium constants for water-gas, hydrogasification and methane
 213 reforming reactions. The system is solved with the Newton-Raphson method.

$$\left\{ \begin{array}{l} n_{CO} + n_{CO_2} + n_{CH_4} + n_{tar} - 1 = 0 \\ 2n_{H_2} + 2n_{H_2O} + 4n_{CH_4} + pn_{tar} - x - 2w = 0 \\ n_{CO} + 2n_{CO_2} + n_{H_2O} + qn_{tar} - w - 2m - y = 0 \\ K_1 = \frac{n_{CO_2} * n_{H_2}}{n_{CO} * n_{H_2O}} \\ K_2 = \frac{n_{CH_4} * \frac{\dot{n}_{tot, wet}}{\dot{n}_{bio, daf}}}{n_{H_2}^2} \\ K_3 = \frac{n_{CO} * n_{H_2}^3}{\left(\frac{\dot{n}_{tot, wet}}{\dot{n}_{bio, daf}}\right)^2 n_{H_2O} n_{CH_4}} \end{array} \right. \quad (10)$$

214 Once the molar specific amounts of the syngas species are evaluated, it is
 215 possible to solve the thermodynamic energy balance of the system reported
 216 in the following equation:

$$\sum_{j=react} n_j * HF_j^0 = \sum_{i=prod} n_i * (HF_i^0 + \Delta H_{T,i}) \quad (11)$$

217 where n_j [moles] and HF_j^0 [kJ/kmol] are the specific moles amount and
 218 standard heat of formation of the j-th reagent (biomass, air and moisture); n_i
 219 [moles] and HF_i^0 [kJ/kmol] are the specific moles amount and the standard
 220 heat of formation of the i-th product (H_2 , CO , CO_2 , H_2O , CH_4 and N_2) and
 221 $\Delta H_{T,i}$ is the enthalpy difference between any given state and the standard
 222 state for the i-th product. $\Delta H_{T,i}$ can be calculated starting from the specific
 223 heat of the product:

$$\Delta H_{T,i} = \int_{298.15}^T C_p(T) dT = \left| aT + b\frac{T^2}{2} + c\frac{T^3}{3} + d\frac{T^4}{4} \right|_{298.15}^T \quad (12)$$

224 where the coefficient a,b,c and d are defined for each gas by Jarungtham-
 225 machote and Dutta[46]. In order to find the equilibrium temperature T_{new} ,
 226 the system is considered adiabatic and the the Newton-Raphson method is
 227 applied to the equations. If $abs(T - T_{new}) < 0.1$ K then the calculated equi-
 228 librium temperature and molar specific gases amounts are the final results;
 229 otherwise, a new iteration is done in order to satisfy the previous condi-
 230 tion. The model is implemented in Python and the input are the biomass
 231 equivalent molecule, the equivalence ratio ER and the initial temperature.
 232 The temperature input is used only as a starting point for the iterating
 233 system; after few cycles the temperature converges to the ones that satisfy
 234 both the chemical and thermal sub-systems. About the ER, a value of 0.335

is assumed. This value is consistent with air blown gasification parameters [50, 37] and it is confirmed by the low tar content in the syngas. Poplar wood chips properties and gasifier model parameters are summarized in Table 1.

2.3. ZEO module modeling

The zeolite filter is able to reduce the total syngas molar flow of about 20% - 30 % by the adsorption of CO_2 . Zeolite 5A is chosen because it has a great selectivity for carbon dioxide in comparison with the other gases that constitute syngas [38]. The gas adsorption in porous solids has been described by the Langmuir equation [38, 39]:

$$q_i = \frac{q_{mi} * B_i * p_i}{1 + \sum_{j=1}^n B_j * p_j} \quad (13)$$

where q_i [mmol/g] is the adsorbed amount of the component i ; q_{mi} [mmol/g] is the saturation adsorbed amount of the component i ; B_i [1/kPa] is the Langmuir constant of the component i ; p_i [kPa] is the equilibrium partial pressure of the component i ; B_j [1/kPa] is the Langmuir constant of the component j ; p_j [kPa] is the equilibrium partial pressure of the component j ; i and j are the gas species of the syngas. Table 1 reports the Langmuir constants and the saturation adsorbed amounts for Zeolite 5A, while Figure 4 depicts the adsorption trends of the syngas gases as function of pressure. It can be noted the high CO_2 selectivity of the zeolite in comparison with others gases.

The mass of zeolite required for adsorbing all the carbon dioxide of the syngas depends on the molar flow of the dry syngas, its CO_2 molar fraction and kinetic constant of adsorption. The ZEO filter module can be constantly regenerated using a rotary valve packaged into modules as described in [40].

257 The mass of zeolite that needs to be regenerated every cycle with duration
 258 of t_{cycle} can be calculated as follows:

$$m_{zeo} = t_{cycle} * \dot{n}_{DG} * \frac{1 + \sum_{j=1}^n B_j * p_j}{q_{m,CO_2} * B_{CO_2} * p_{ads} * x_{CO_2}} \quad (14)$$

259 where p_{ads} [kPa] is the total pressure of the syngas inside the ZEO filter.
 260 A constant temperature of the zeolite filter and of the inlet syngas of 303 K is
 261 assumed and the pressure of the inlet syngas is set to 500 kPa as suggested in
 262 [38, 39]. The cycling time of regeneration depends on kinetic CO_2 adsorption
 263 constant. In this study a plausible time of 60 seconds is assumed and future
 264 work will investigate this aspect. Zeolites adsorption generates heat, Ranjani
 265 et al. [51] suggests that 64-70 kJ are released for every mole of CO_2 adsorbed.
 266 This heat needs to be discharge by the ZEO module in order to keep the
 267 temperature constant at 303 K. In this preliminary study, no attention was
 268 paid to the ZEO module heat balance. Furthermore, the gas filtering sub-
 269 system considered in this work is based on the power plant described by
 270 Allesina et al. [50]. It was designed with the idea of coupling the gasifier with
 271 an internal combustion engine. Since the minimum presence of tars could
 272 negatively affect the performance of the zeolite adsorber, syngas purification
 273 unit should be properly designed. A potential alternative to water scrubber
 274 is oil scrubber with subsequent stripping of tars [52, 53].

275 2.4. Compressor and storage system modeling

276 The modeling of the syngas compression is carried out considering it as
 277 a polytropic transformation. The electrical power required for compression
 278 is given by Pedrazzi et al. [54]:

$$P_{comp} = \frac{\dot{n}_{gas} L_{comp, is}}{\eta_{comp}} = \frac{\dot{n}_{gas}}{\eta_{comp}} \frac{z R T_{in}}{z - 1} \left[1 - \left(\frac{p_{out}}{p_{in}} \right)^{\frac{z-1}{z}} \right] \quad (15)$$

where z is the polytrophic coefficient, R is the universal gas constant equal to $8.314 \text{ J mol}^{-1} \text{ K}^{-1}$, T_{in} is the gas inlet temperature (25°C for syngas compressor 1 and 30°C for syngas compressor 2), p_{in} and p_{out} [atm] are the gas inlet and outlet pressures, \dot{n}_{gas} [mol/s] is the gas molar flow and η_{comp} is the compressor efficiency available from manufacturer's data [54]. The maximum pressure value inside the storage system is a fundamental parameter required to **design the tanks and the compressor properly**. Assuming ideal gas and a constant syngas storage temperature $T_s = 25^\circ\text{C}$, the pressure inside the tanks is calculated by the ideal gas law:

$$p_s = \frac{n R T_s}{V} \quad (16)$$

where n [mol] are the moles of syngas inside the tanks and V [m^3] is the storage total volume. Assuming a value of the initial syngas moles n_{in} inside the storage, the moles of syngas at the time τ [s] are given by:

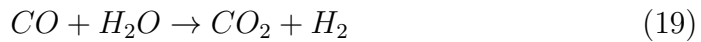
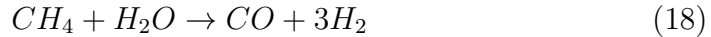
$$n = n_{in} + \int_0^\tau (\dot{n}_{in,s}(t) - \dot{n}_{out,s}(s)) dt \quad (17)$$

where $\dot{n}_{in,s}(t)$ and $\dot{n}_{out,s}(t)$ [mol/s] are the inlet and the outlet molar flow at the instantaneous time t [s]. Table 2 reports the model parameters of the storage and compressor sub-systems. The total volume of storage and the initial syngas amount in the tank are reduced of about 50% in comparison with the conventional system without PPO and ZEO modules as investigated in [55, 56]. This result is reached thanks to the PPO adoption that decreases

the molar flow of dry syngas of about the 20% - 30%, while the filtration in the ZEO module further reduces the syngas molar flow of about another 20% - 30% as shown in the results.

2.5. SOFC modeling

The SOFC model used in this study is based on the work of Bang-Møller and Rokni [18]. This model does not take into account the recirculation of gas at the cell anode. This feature may strongly compromise the fuel cell efficiency in case of the presence of gases that do not take part in the electro-chemical, shift and reforming reactions. Unfortunately, syngas contains considerable amounts of CO_2 and N_2 . To overcome this issue, the model previously cited is implemented with the reforming model presented by Rami Salah El-Emam et al. [22]. As described by Rami Salah El-Emam, the electro-chemical reactions take place in both the anode and the cathode of the cell (Eq.22), while the reforming and the monoxide water shift occur only near the anode (Eqs. 18, 19). Equation 22 presents the overall electro-chemical reaction that is divided into two sub-reactions: the hydrogen reacts with the oxygen ions to form water and electrons according to Eq. 20 at the anode, while, at the cathode, the oxygen from inlet air reacts with the electrons from the anode (Eq. 21) to form oxygen ions that flow to the anode through the solid oxide electrolyte.





317 The mathematical modeling of reforming and electrochemical reactions
 318 is explained in References [22] and [18]. Using these models, it is possible
 319 to calculate the electrical power production and the electrical conversion
 320 efficiency for a given syngas inlet flow with a specific composition. The
 321 SOFC model parameters adopted in the simulations are reported in Table 2.

322 2.6. MGT modeling

323 Mathematical description of gas turbines is well described in literature.
 324 Details and assumptions of the present model can be found in Bang-Møller
 325 and Rokni work [18]. Characteristics of the turbine and others components
 326 connected to the MGT are listed in Table 2.

327 3. Simulation results and discussion

328 In this work four different cases are simulated. First of all, the basic
 329 system composed of a downdraft gasifier, a storage tank and a SOFC-MGT
 330 is simulated. After this step, the two possible solutions consisting of N_2
 331 purging from air or CO_2 separation from syngas are discussed separately.
 332 Finally, the complete system provided with PPO module and ZEO module
 333 is simulated.

3.1. Case I (Gasifier + SOFC + MGT)

The SOFC-MGT unit constantly produces energy all over the year of simulation in order to preserve the stability of the cells and their gaskets, which are very sensitive to thermal stresses [57]. The syngas molar flow consumed by the SOFC-MGT unit is calculated by Equation 23 that considers the cycling working of the DG:

$$\dot{n}_{syngas-SOFC} = \frac{h_{operation}\dot{n}_{DG}}{h_{operation} + h_{maintenance}} \quad (23)$$

Figure 5 depicts the overall model implemented in Matlab SimulinkTM software environment. Table 3 reports the simulation results. Gasifier cold efficiency is about 79%, this value is confirmed by literature that suggests an efficiency of 70% - 80% for air-blown downdraft gasifier [37, 4, 44]. Syngas composition consists of about 19% vol. of H_2 and 15% vol. of CO , the higher heating value of 4.75 MJ/Nm^3 is similar to the results reported by Basu [37] for this kind of gasifier. SOFC-MGT unit has a constant electrical power production of 197.43 kW all over the simulated year. The auxiliary consumption of the whole system strongly depends on tank pressurization level. The average annual value is 34.24 kW. For this reason, the net average power production is reduced to 163.19 kW and the electrical efficiency of the system is 25.43%.

3.2. Case II (PPO + Gasifier + SOFC + MGT)

Table 4 shows the results of the simulation of the system previously described and now equipped with the PPO module. The oxygen enriched air

356 flow is about 1.27 mol/s. This value is lower than 2.94 mol/s obtained with-
 357 out PPO membrane (Case I). Syngas composition is consistent with the work
 358 of Wang et al. [58], where oxygen-enriched air (50% oxygen and 50% nitro-
 359 gen) is used as gasifying agent in a double stage downdraft gasifier fueled
 360 with pine sawdust pellets. Differences of 1-2% between the model outputs
 361 and Wang's results about CO and H_2 contents are achieved (29% vs. 27%
 362 for H_2 and 26% Vs. 25% for CO). The gasification with oxygen-enriched air
 363 assures high gasifier performance in terms of cold gas efficiency (92%), tar
 364 production (0.27 g/Nm³) and syngas higher heating value (7.55 MJ/Nm³).
 365 The syngas outlet flow is 3.589 mol/s, consistently lower than Case I where
 366 syngas flow is 5.01 mol/s. The average equilibrium temperature of gasifi-
 367 cation in this case is 931 K. This value is only 36 K higher than Case I.
 368 Wang et al.[58] suggestes a peak temperature of about 1200 K with oxygen-
 369 enriched air. With this temperature, conventional material adopted in air
 370 gasifier can be used (i.e. stainless steel and refractory brick [2, 6]). In Case
 371 II, the overall net power production is 210.52 kW and the electrical efficiency
 372 is boosted to 32.81%. The average auxiliary consumption is 42 kW, 8 kW
 373 higher than Case I. This is due to the PPO module that uses air at 1 MPa
 374 pressure generated by an air compressor. The electrical consumption of the
 375 air compressor is 15.3 kW and it is fully compensated by the increasing of
 376 the gasifier efficiency and the SOFC-MGT unit efficiency.

377 3.3. Case III (*Gasifier + ZEO + SOFC + MGT*)

378 Table 5 resumes the simulation results of the system with the ZEO fil-
 379 tering module instead of PPO membrane. The filtered syngas has a higher
 380 heating value of 5.9 MJ/Nm³. This value falls between Case I (4.75 MJ/Nm³)

381 and Case II (7.55 MJ/Nm³). The pressure of the storage tank ranges between
 382 0.267-0.488 MPa, similar to the values obtained in Case II (0.266-0.462 MPa)
 383 and Case I (0.267-0.539 MPa). The zeolite mass required to perform con-
 384 tinuously the filtration is 23.742 kg. The value obtained is consistent with
 385 Tagliabue et al. work [40]. However, in future work, the CO_2 adsorbed by
 386 the ZEO module can be stored in order to create a carbon sequestration sys-
 387 tem. The power production and the net electrical efficiency of the system is
 388 low (148.74 kW of power production and 22.87% of electrical efficiency) as a
 389 consequence of the energy absorbed by the syngas compressor 1 (see Figure
 390 1) to increase the pressure of the syngas to 0.5 MPa before the ZEO module.
 391 This electrical energy consumption is higher than Cases II and I, in addition
 392 the efficiency of the SOFC-MGT module fueled with the filtered syngas is
 393 lower. As shown in Table 5, the SOFC-MGT efficiency in Case III is about
 394 34%, thus lower than Case II (42.08%) and Case I (37.46%).

395 3.4. Case IV (PPO + Gasifier + ZEO + SOFC + MGT)

396 The results about the fully equipped gasifier power system are reported
 397 in Table 6. A high power production (194.53 kW) and electrical efficiency
 398 (30.32%) is reached thanks to the high H_2 and CO amounts in the filtered
 399 syngas. In fact, the H_2 volume percentange reaches 41.53% and the CO
 400 volume percentange is boosted to 32.54%. As a consequence of this com-
 401 position, the higher heating value of the syngas is 10.19 MJ/Nm³, a value
 402 typical for oxygen-blown gasifiers [37]. Therefore, the SOFC-MGT unit syn-
 403 gas consumption is 2.696 mol/s. This value is about 45% lower than Case I
 404 (4.95 mol/s), 24% lower than Case II (3.545 mol/s) and 33% lower than Case
 405 III (4.02 mol/s). A pressure range of 0.266-0.415 MPa is achieved. In this

case power production and efficiency is lower than Case II as result of higher average auxiliary consumption (51.80 kW) and lower SOFC-MGT unit efficiency (38.41%). However, the utilization of the ZEO module has several advantages: separates the CO_2 and reduces the storage peaks pressure.

3.5. Performance and energy considerations

Figure 6 shows the electrical efficiency and the average power production in every scenario. Case II resulted the best in terms of energy conversion; the overall electrical efficiency reaches 32% and the power production is about 210 kW. These values are higher than commercial gasification power systems with internal combustion engines where the maximum electrical efficiency hardly reaches 25% [37, 4, 2]. This result is given by the PPO module that increases the gasifier efficiency to 92% (75% is the reference value for air blown gasifier [37]) and the SOFC-MGT module which has a higher electrical conversion efficiency (about 42%) compared to common engine-alternator generator units (about 27% [4, 59, 3]). Case II is the best in terms of energy balance as shown in Figure 7. These graphs do not consider the thermal energy that can be recovered from the gasifier or the SOFC-MGT unit. The highest energy loss occurs at the SOFC-MGT unit (about 52%), while auxiliary consumption of the blowers and the auxiliary equipment of the gasifier are low (9%). In Cases I and III, the low efficiency of the gasifier reduces the overall electrical performance of the system. In Cases III and IV the ZEO module consumes energy to separate the CO_2 from the gas, however no efficiency increase occurs in the SOFC-MGT unit with a CO_2 free syngas and the final result is a lower power production. The system modeled in this work is obtained starting from a reference power plant described by Allesina et. al

[50] where IC engines are used instead of the SOFC-MGT unit. The author reports an experimental cold gasification efficiency of 67%. Considering an electrical IC engine-alternator unit efficiency of about 27%, as suggested by Puglia et al. [3], the total electrical efficiency is about 18%. This value is 30% lower than Case I and it is 45% lower than Case II. Another study made by Patuzzi et al. [60] reports the values of the net electrical efficiency of three different commercial biomass gasifier - IC engine power plants. The average efficiency is about 20%, this value is consistent with the one obtained for Allesina et al. [50].

4. Conclusions

The biomass fueled system with PPO module (Case II) shows the higher electrical efficiency of about 33%. The reasons behind this result are various. First of all, oxygen-enriched air boosts the gasifier cold efficiency from 79% (Case I with air) to 92% (Cases II and IV with oxygen-enriched air). In addition, the SOFC-MGT unit presents a higher efficiency (about 42%) compared to IC engine-alternator unit (about 27%), ORC cycle (about 20%) or EFGT cycle (about 20%). In Cases III and IV, the zeolites adsorption module consumes energy to increase the higher heating value of the syngas but not the performance of the SOFC-MGT system, this reduces the overall system efficiency. The energy balances of four cases investigated show that the greater losses are in the SOFC-MGT unit. This unit has the difficult task to convert the chemical energy of a gas fuel into electrical energy in an efficient way. An efficiency of about 50% is reached with natural gas, in this study the maximum electrical efficiency is about 42% using a syngas

455 produced with an oxygen-enriched air as gasifying agent. This difference is
 456 given by the presence of several inert gases into the syngas that reduces the
 457 electrochemical conversion of the SOFC. The removal or the conversion of
 458 these gases into syntethic natural gases (SNG) is possible and, in this way,
 459 the efficiency of the SOFC-MGT unit will be similar to the value reach for
 460 natural gas one. But, cost and energy self-consumption of the upgrading
 461 process are very high and not convenient for this kind of power plants. Cases
 462 III and IV has a lower efficiency compared to Case II, however, with the
 463 ZEO module, it is possible to sepearate the CO_2 content of the syngas with
 464 environmental benefits in case the module is coupled with a CO_2 sequestra-
 465 tion system. Future work will consider exergy calculations and experimental
 466 tests on a micro-scale power system (5-20 kW of electrical power) with PPO
 467 module and SOFC module in order to validate modeling results and to assest
 468 system durability. In addition, economical net present value analysis will be
 469 done to estimate the economic sustainability of the power plant.

470 **Nomenclature**

471 \dot{m} mass flow [kg/s]

472 \dot{n} molar flow [mol/s]

473 τ time [s]

474 ASH ash content of the biomass [%]

475 B Langmuir constant [1/kPa]

476 C carbon

477	C_p	specific heat [J/(mol K)]
478	DG	downdraft gasifier
479	e	electron
480	$EFGT$	external firing gas turbine
481	ER	equivalence ratio [ad]
482	H	hydrogen
483	H_T	enthalpy [kJ/kmol]
484	HF^0	standard heat of formation [kJ/kmol]
485	HHV	higher heating value [MJ/Nm ³ or MJ/kg]
486	IC	internal combustion
487	K	equilibrium constant [ad]
488	L	work [kJ]
489	M	total moisture content of the biomass [%]
490	m	specific molar amount of oxygen [mol/mol_{bio}]
491	m_{tar, Nm^3}	volumetric tar amount [g/Nm^3]
492	$MCFC$	molten carbonate fuel cell
493	MGT	micro gas turbine
494	MW	molecular weight [g/mol]

495	N	nitrogen
496	n	specific molar amount of gases and tar [mol/mol_{bio}]
497	O	oxygen
498	ORC	organic rankine cycle
499	P	power [kW]
500	p	pressure [atm]
501	$PDSM$	polydimethylsiloxan
502	PPO	polyphenylene oxide
503	Q	molar flow [mol/s]
504	q	adsorbed amount [mmol/g]
505	R	universal gas constant [J/(mol K)]
506	$SOFc$	solide oxide fuel cell
507	T	temperature [K]
508	t	time [s]
509	V	volume [m ³]
510	w	specific molar amount of biomass moisture [mol/mol_{bio}]
511	x	molar fraction
512	y	molar fraction

513	z	polytrophic coefficient
514	ZEO	zeolite
515	α	selectivity
516	Δ	difference
517	γ	permeability [$\text{mol m}^{-2} \text{s}^{-1} \text{bar}^{-1}$]
518	ϕ	pressure ratio
519	Subscripts	
520	ads	adsorption
521	ar	as received
522	bio	biomass
523	$comp$	compressor
524	daf	dry ash free
525	db	dry basis
526	g	gas
527	in	inlet
528	m	saturation
529	out	outlet
530	P	permeate

531 p hydrogen coefficient of tar

532 $prod$ product

533 q oxygen coefficient of tar

534 R retentate

535 $react$ reactant

536 s storage

537 x hydrogn coefficient of the biomass

538 y hydrogen coefficient of the biomass

539 z nitrogen coefficient of the biomass

540 **References**

- 541 [1] IEA. Technology roadmap - bioenergy for heat and power. Technical
542 report, IEA, 2012.
- 543 [2] Thomas B. Reed and Agua Das. *Handbook of Biomass Downdraft Gasi-*
544 *fier Engine Systems*. The biomass energy foundation press, 1988.
- 545 [3] G. Allesina, S. Pedrazzi M.Puglia, and P. Tartarini. Upgrading or sub-
546 stituting the gasification process for electrical energy production: an
547 energy-based comparison. In *XXX UIT Conference, Bologna 2012*, 2012.
- 548 [4] H.A.M. Knoef. *Handbook of Biomass Gasification*. BTG, 2005.

- 549 [5] Amitava Datta, Ranjan Ganguly, and Luna Sarkar. Energy and exergy
550 analyses of an externally fired gas turbine (efgt) cycle integrated with
551 biomass gasifier for distributed power generation. *Energy*, 35(1):341 –
552 350, 2010.
- 553 [6] FAO Forestry Department Mechanical Wood Products Branch. *Woodgas
554 as engine fuel*, volume ISBN 92-5-102436-7. F.A.O., 1986.
- 555 [7] F. Martelli, G. Riccio, S. Maltagliati, and D. Chiaramonti. Technical
556 study and environmental impact of an external fired gas turbine power
557 plant fed by solid fuel. *1st world Conference of Biomass, Sevilla*, 2000.
- 558 [8] V. Naso. *La macchina di Stirling*. CEA, 1991.
- 559 [9] C. Souleymane. Motori a combustione interna e turbine a gas di pic-
560 cola taglia per gas di sintesi. Master’s thesis, Università degli Studi di
561 Padova, Italy., 2012.
- 562 [10] Farqad Al-Hadeethi, Moh’d Al-Nimr, and Mohammad Al-Safadi. Us-
563 ing the multiple regression analysis with respect to {ANOVA} and 3d
564 mapping to model the actual performance of {PEM} (proton exchange
565 membrane) fuel cell at various operating conditions. *Energy*, 90, Part
566 1:475 – 482, 2015.
- 567 [11] Guido Galeno. *Modellizzazione di un micro cogeneratore basato sulla
568 tecnologia mcfc accoppiata ad un gassificatore di biomassa*. PhD thesis,
569 University of Cassino, Italy, 2006-2007.
- 570 [12] Giulio Donolo, Giulio De Simon, and Maurizio Fermeglia. Steady

- state simulation of energy production from biomass by molten carbonate fuel cells. *Journal of Power Sources*, 158(2):1282 – 1289, 2006.
- Special issue including selected papers from the 6th International Conference on Lead-Acid Batteries (LABAT 2005, Varna, Bulgaria) and the 11th Asian Battery Conference (11 ABC, Ho Chi Minh City, Vietnam) together with regular papers.
- [13] Stefano Cordiner, Massimo Feola, Vincenzo Mulone, and Fabio Romanelli. Analysis of a {SOFC} energy generation system fuelled with biomass reformat. *Applied Thermal Engineering*, 27(4):738 – 747, 2007.
- Energy: Production, Distribution and Conservation.
- [14] E. Achenbach. Three-dimensional and time-dependent simulation of a planar solid oxide fuel cell stack. *Journal of Power Sources*, 49:333–348, 1994.
- [15] M. Mortazaei and M. Rahimi. A comparison between two methods of generating power, heat and refrigeration via biomass based solid oxide fuel cell: A thermodynamic and environmental analysis. *Energy Conversion and Management*, 126:132 – 141, 2016.
- [16] F. Calise, M. Dentice d’Accadia, A. Palombo, and L. Vanoli. Simulation and exergy analysis of a hybrid solid oxide fuel cell (sofc)–gas turbine system. *Energy*, 31(15):3278 – 3299, 2006. {ECOS} 2004 - 17th International Conference on Efficiency, Costs, Optimization, Simulation, and Environmental Impact of Energy on Process Systems 17th International Conference on Efficiency, Costs, Optimization, Simulation, and Environmental Impact of Energy on Process Systems.

- 595 [17] L. Fryda, K.D. Panopoulos, and E. Kakaras. Integrated {CHP} with
596 autothermal biomass gasification and sofc-mgt. *Energy Conversion and*
597 *Management*, 49(2):281 – 290, 2008.
- 598 [18] C. Bang-Moller and M. Rokni. Thermodynamic performance study of
599 biomass gasification, solid oxide fuel cell and micro gas turbine hybrid
600 systems. *Energy Conversion and Management*, 51(11):2330 – 2339, 2010.
- 601 [19] Made Sucipta, Shinji Kimijima, and Kenjiro Suzuki. Performance anal-
602 ysis of the sofc-mgt hybrid system with gasified biomass fuel. *Journal*
603 *of Power Sources*, 174(1):124 – 135, 2007. jce:titlejHybrid Electric Ve-
604 hiclesj/ce:titlej.
- 605 [20] Pegah Ghanbari Bavarsad. Energy and exergy analysis of internal re-
606 forming solid oxide fuel cellâ“gas turbine hybrid system. *International*
607 *Journal of Hydrogen Energy*, 32(17):4591 – 4599, 2007. Fuel Cells.
- 608 [21] C. Ozgur Colpan, Ibrahim Dincer, and Feridun Hamdullahpur. Thermo-
609 dynamic modeling of direct internal reforming solid oxide fuel cells oper-
610 ating with syngas. *International Journal of Hydrogen Energy*, 32(7):787
611 – 795, 2007. jce:titlejFuel Cellsj/ce:titlej.
- 612 [22] Rami Salah El-Emam, Ibrahim Dincer, and Greg F. Naterer. Energy
613 and exergy analyses of an integrated {SOFC} and coal gasification sys-
614 tem. *International Journal of Hydrogen Energy*, 37(2):1689 – 1697, 2012.
615 jce:titlej10th International Conference on Clean Energy 2010j/ce:titlej.
- 616 [23] Penyarat Chinda and Pascal Brault. The hybrid solid oxide fuel cell

- 617 (sofc) and gas turbine (gt) systems steady state modeling. *International*
618 *Journal of Hydrogen Energy*, 37(11):9237 – 9248, 2012.
- 619 [24] S.H. Chan, H.K. Ho, and Y. Tian. Modelling of simple hybrid solid
620 oxide fuel cell and gas turbine power plant. *Journal of Power Sources*,
621 109(1):111 – 120, 2002.
- 622 [25] Tae Won Song, Jeong Lak Sohn, Jae Hwan Kim, Tong Seop Kim,
623 Sung Tack Ro, and Kenjiro Suzuki. Performance analysis of a tubu-
624 lar solid oxide fuel cell/micro gas turbine hybrid power system based on
625 a quasi-two dimensional model. *Journal of Power Sources*, 142(1â“2):30
626 – 42, 2005.
- 627 [26] Mahsa Aghaie, Mehdi Mehrpooya, and Fathollah Pourfayaz. Introduc-
628 ing an integrated chemical looping hydrogen production, inherent carbon
629 capture and solid oxide fuel cell biomass fueled power plant process con-
630 figuration. *Energy Conversion and Management*, 124:141 – 154, 2016.
- 631 [27] Masood Ebrahimi and Iraj Moradpoor. Combined solid oxide fuel cell,
632 micro-gas turbine and organic rankine cycle for power generation (sofc-
633 mgt-orc). *Energy Conversion and Management*, 116:120 – 133, 2016.
- 634 [28] Ph. Hofmann, K.D. Panopoulos, P.V. Aravind, M. Siedlecki,
635 A. Schweiger, J. Karl, J.P. Ouweltjes, and E. Kakaras. Operation of
636 solid oxide fuel cell on biomass product gas with tar levels $>10 \text{ g}$
637 nm^3 . *International Journal of Hydrogen Energy*, 34(22):9203 – 9212,
638 2009.

- 639 [29] Lopamudra Devi, Krzysztof J Ptasinski, and Frans J.J.G Janssen. A re-
640 view of the primary measures for tar elimination in biomass gasification
641 processes. *Biomass and Bioenergy*, 24(2):125–140, 2003.
- 642 [30] Jinsong Zhou, Qing Chen, Hui Zhao, Xiaowei Cao, Qinfeng Mei,
643 Zhongyang Luo, and Kefa Cen. Biomass–oxygen gasification in a high-
644 temperature entrained-flow gasifier. *Biotechnology Advances*, 27(5):606
645 – 611, 2009. Bioenergy Research & Development in ChinaICBT
646 2008.
- 647 [31] T. Melin and R. Rautenbach. *Membranverfahren, Grundlagen der*
648 *Modul- und Anlagenauslegung*. 2007.
- 649 [32] K.C. Khulbe, T. Matsuura, G. Lamarche, and H.J. Kim. The morphol-
650 ogy characterisation and performance of dense ppo membranes for gas
651 separation. *Journal of Membrane Science*, 135(2):211 – 223, 1997.
- 652 [33] Janusz Kotowicz and Adrian Balicki. Enhancing the overall efficiency
653 of a lignite-fired oxyfuel power plant with {CFB} boiler and membrane-
654 based air separation unit. *Energy Conversion and Management*, 80:20
655 – 31, 2014.
- 656 [34] Giacomo Bisio, Alessandro Bosio, and Giuseppe Rubatto. Thermody-
657 namics applied to oxygen enrichment of combustion air. *Energy Con-*
658 *version and Management*, 43(18):2589 – 2600, 2002.
- 659 [35] H. Scott Coombe and Sen Nieh. Polymer membrane air separation per-
660 formance for portable oxygen enriched combustion applications. *Energy*
661 *Conversion and Management*, 48(5):1499 – 1505, 2007.

- [36] Yanhong Hao, Yi Huang, Minhui Gong, Wenying Li, Jie Feng, and Qun Yi. A polygeneration from a dual-gas partial catalytic oxidation coupling with an oxygen-permeable membrane reactor. *Energy Conversion and Management*, 106:466 – 478, 2015.
- [37] Prabir Basu. *Biomass Gasification and Pyrolysis: Practical Design and Theory*. Academic Press, Elsevier, 2010.
- [38] Saeed Pakseresht, Mohammad Kazemeini, and Mohammad M. Akbarnejad. Equilibrium isotherms for co, co₂, {CH₄} and {C₂H₄} on the 5a molecular sieve by a simple volumetric apparatus. *Separation and Purification Technology*, 28(1):53 – 60, 2002.
- [39] Gi-Moon Nam, Byung-Man Jeong, Seok-Hyun Kang, Byung-Kwon Lee, and Dae-Ki Choi. Equilibrium isotherms of ch₄, c₂h₆, c₂h₄, n₂, and h₂ on zeolite 5a using a static volumetric method. *Journal of Chemical & Engineering Data*, 50(1):72–76, 2005.
- [40] Marco Tagliabue, David Farrusseng, Susana Valencia, Sonia Aguado, Ugo Ravon, Caterina Rizzo, Avelino Corma, and Claude Mirodatos. Natural gas treating by selective adsorption: Material science and chemical engineering interplay. *Chemical Engineering Journal*, 155(3):553 – 566, 2009.
- [41] Zoltán Bacsik, Ocean Cheung, Petr Vasiliev, and Niklas Hedin. Selective separation of {CO₂} and {CH₄} for biogas upgrading on zeolite naka and sapo-56. *Applied Energy*, 162:613 – 621, 2016.

- 684 [42] Mariem Kacem, Mario Pellerano, and Arnaud Delebarre. Pressure swing
685 adsorption for CO_2/N_2 and CO_2/CH_4 separation: Comparison between ac-
686 tivated carbons and zeolites performances. *Fuel Processing Technology*,
687 138:271 – 283, 2015.
- 688 [43] Qassim Hassan Dirar and Kevin F. Loughlin. Intrinsic adsorption prop-
689 erties of CO_2 on 5a and 13x zeolite. *Adsorption*, 19(6):1149–1163, 2013.
- 690 [44] Niladri Sekhar Barman, Sudip Ghosh, and Sudipta De. Gasification of
691 biomass in a fixed bed downdraft gasifier – a realistic model including
692 tar. *Bioresource Technology*, 107:505–511, 2012.
- 693 [45] Takashi Yamazaki, Hirokazu Kozu, Sadamu Yamagata, Naoto Murao,
694 Sachio Ohta, Satoru Shiya, and Tatsuo Ohba. Effect of superficial ve-
695 locity on tar from downdraft gasification of biomass. *Energy & Fuels*,
696 19:1186–1191, 2005.
- 697 [46] S. Jarungthammachote and A. Dutta. Thermodynamic equilibrium
698 model and second law analysis of a downdraft waste gasifier. *Energy*,
699 32(9):1660 – 1669, 2007.
- 700 [47] Giulio Allesina, Simone Pedrazzi, Luca Guidetti, and Paolo Tartarini.
701 Modeling of coupling gasification and anaerobic digestion processes for
702 maize bioenergy conversion. *Biomass and Bioenergy*, 81:444 – 451, 2015.
- 703 [48] Giulio Allesina, Simone Pedrazzi, Federico Sgarbi, Elisa Pompeo,
704 Camilla Roberti, Vincenzo Cristiano, and Paolo Tartarini. Approaching
705 sustainable development through energy management, the case of fongo

- 706 tongo, cameroon. *International Journal of Energy and Environmental*
707 *Engineering*, 6(2):121–127, 2014.
- 708 [49] Giulio Allesina, Simone Pedrazzi, Emma La Cava, Michele Orlandi,
709 Miriam Hanuskova, Caludio Fontanesi, and Paolo Tartarini. Energy-
710 based assessment of optimal operating parameters for coupled biochar
711 and syngas production in stratified downdraft gasifiers. In *International*
712 *Heat Transfer Conference 15, Kyoto, Japan*, 2014.
- 713 [50] Giulio Allesina, Simone Pedrazzi, and Paolo Tartarini. Modeling and
714 investigation of the channeling phenomenon in downdraft stratified
715 gasifiers. *Bioresource Technology*, 146(0):704 – 712, 2013.
- 716 [51] Ranjani V. Siriwardan, Ming-Shing Shen, and Edward P. Fisher. Ad-
717 sorption of co2 on zeolites at moderate temperatures. *Energy and Fuels*,
718 19:1153–1159, 2005.
- 719 [52] Thana Phuphuakrat, Tomoaki Namioka, and Kunio Yoshikawa. Absorp-
720 tive removal of biomass tar using water and oily materials. *Bioresource*
721 *Technology*, 102(2):543–549, 2011.
- 722 [53] Shunsuke Nakamura, Shigeru Kitano, and Kunio Yoshikawa. Biomass
723 gasification process with the tar removal technologies utilizing bio-oil
724 scrubber and char bed. *Applied Energy*, 170:186 – 192, 2016.
- 725 [54] S. Pedrazzi, G. Zini, and P. Tartarini. Complete modeling and soft-
726 ware implementation of a virtual solar hydrogen hybrid system. *Energy*
727 *Conversion and Management*, 51(1):122 – 129, 2010.

- 728 [55] Simone Pedrazzi, Giulio Allesina, Alberto Muscio, and Paolo Tartarini.
729 Modeling and simulation of a dg-sofc-mgt hybrid system. In *7° Con-*
730 *gresso Nazionale AIGE, Rende (CZ) Italy*, 2013.
- 731 [56] Simone Pedrazzi. *Modeling and optimization of advanced systems for*
732 *electrical energy production from wood biomass*. PhD thesis, HIGH ME-
733 CHANICS AND AUTOMOTIVE DESIGN & TECHNOLOGY, Univer-
734 sity of Modena and Reggio Emilia, Dep. of Engineering 'Enzo Ferrari',
735 2013.
- 736 [57] DOE. *Fuel Cell Handbook (Seventh Edition)*. 2004.
- 737 [58] Zhiqi Wang, Tao He, Jianguang Qin, Jingli Wu, Jianqing Li, Zhongyue
738 Zi, Guangbo Liu, Jinhui Wu, and Li Sun. Gasification of biomass with
739 oxygen-enriched air in a pilot scale two-stage gasifier. *Fuel*, 150:386 –
740 393, 2015.
- 741 [59] H.A.M. Knoef. *Handbook of Biomass Gasification, Second Edition*.
742 BTG, 2012.
- 743 [60] Francesco Patuzzi, Dario Prando, Stergios Vakalis, Andrea Maria Rizzo,
744 David Chiaramonti, Werner Tirler, Tanja Mimmo, Andrea Gasparella,
745 and Marco Baratieri. Small-scale biomass gasification {CHP} systems:
746 Comparative performance assessment and monitoring experiences in
747 south tyrol (italy). *Energy*, 112:285 – 293, 2016.
- 748 [61] S. Pedrazzi, G. Allesina, and P. Tartarini. Aige conference: A kinetic
749 model for a stratified downdraft gasifier experimental assessment and

750 modeling of energy conversion effectiveness in a gasification power plant.
751 *International Journal of Heat and Technology*, 30(1):41–44, 2012.

752 **Figure captions and tables**

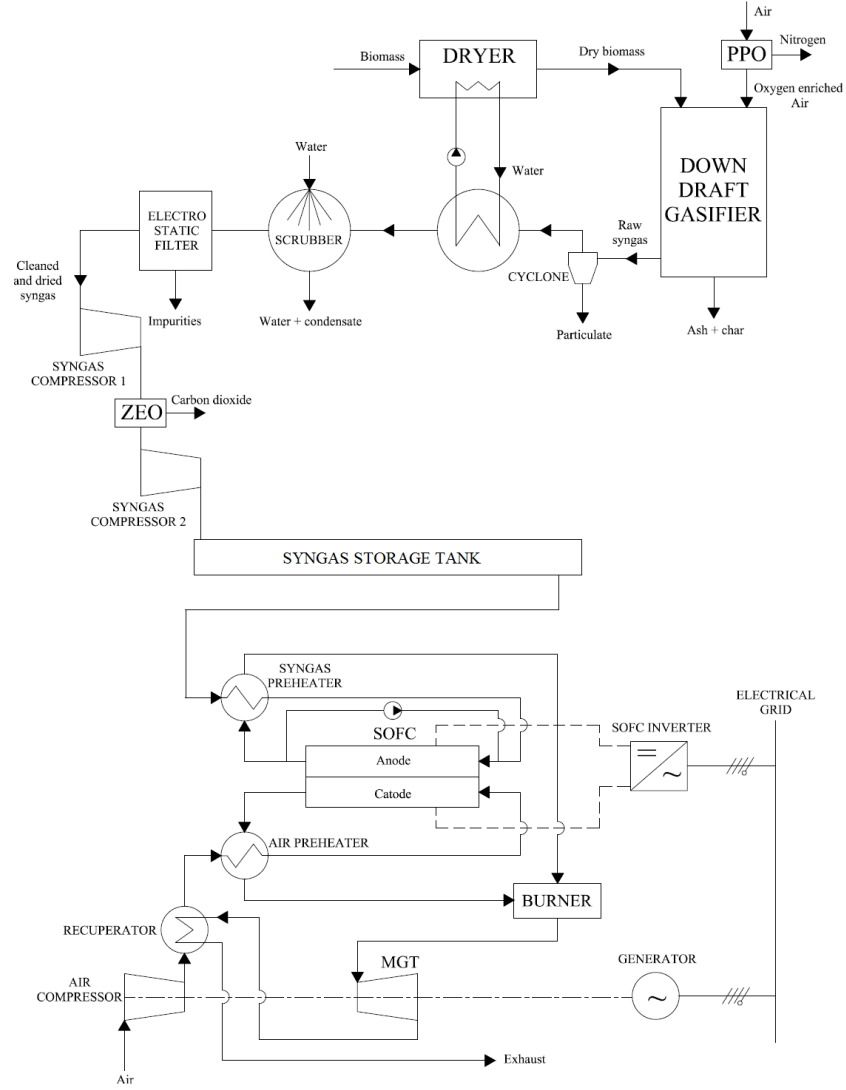


Figure 1: DG-SOFC-MGT hybrid system with zeolite CO_2 adsorption and oxygen-enriched air layout

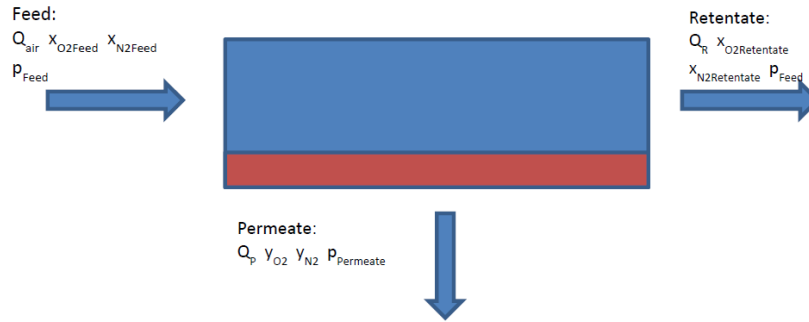


Figure 2: Oxygen enriched air membrane separator principle

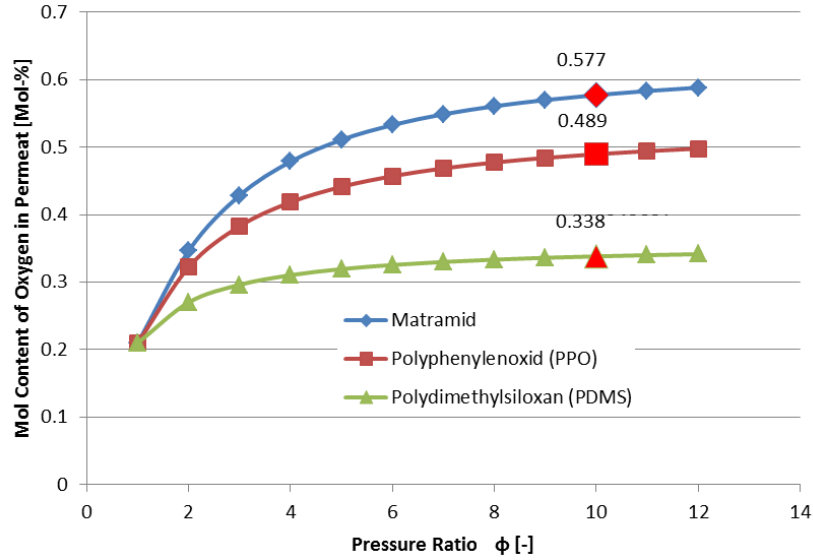


Figure 3: Characteristics of the separation membranes

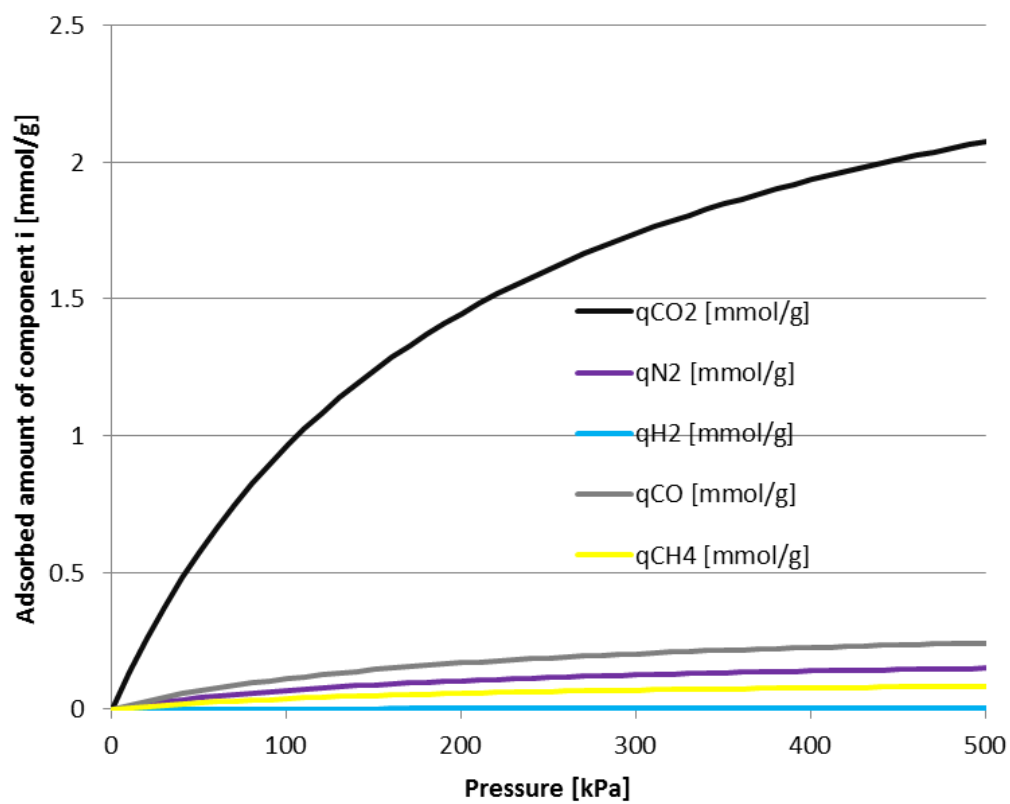


Figure 4: Zeolite 5A adsorbing curve Vs. pressure

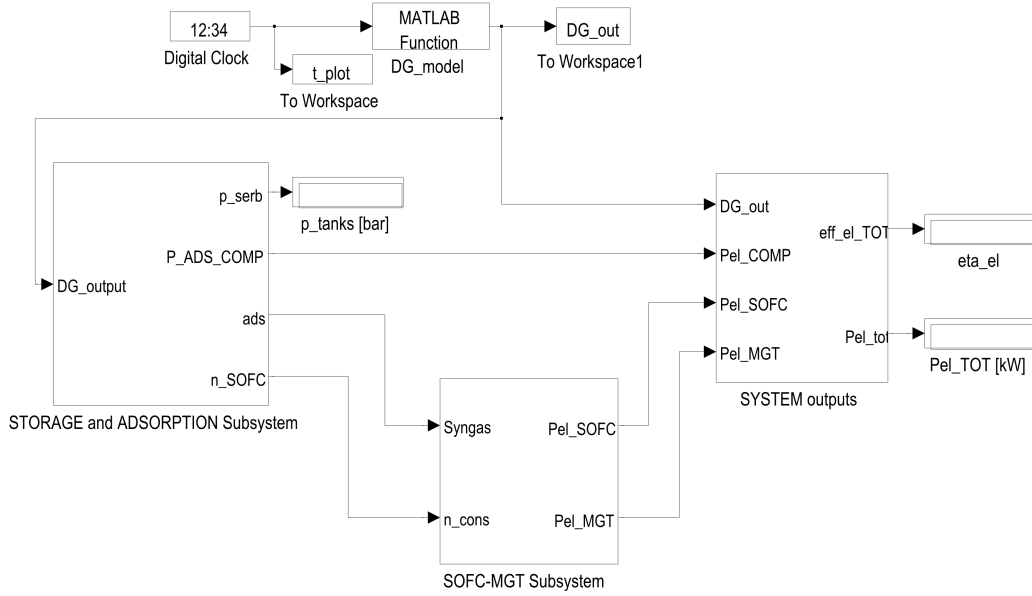


Figure 5: DG-SOFC-MGT hybrid system with zeolite CO_2 adsorption and oxygen-enriched air implemented in Matlab SimulinkTM

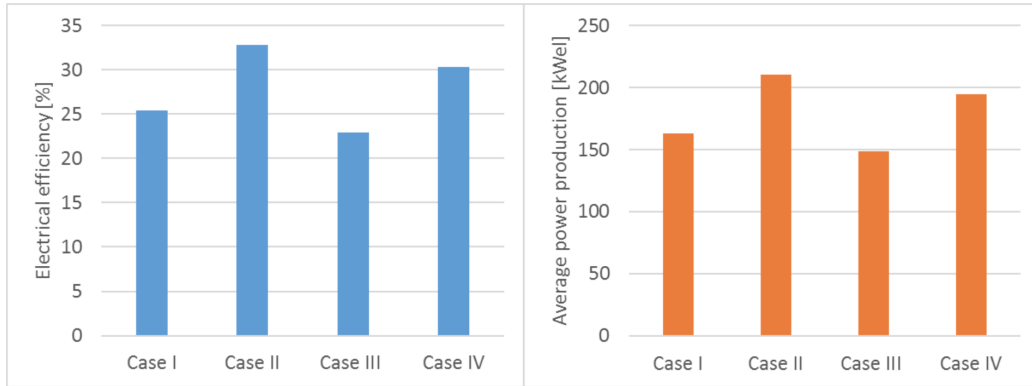


Figure 6: Efficiencies and electrical production values of the studied cases

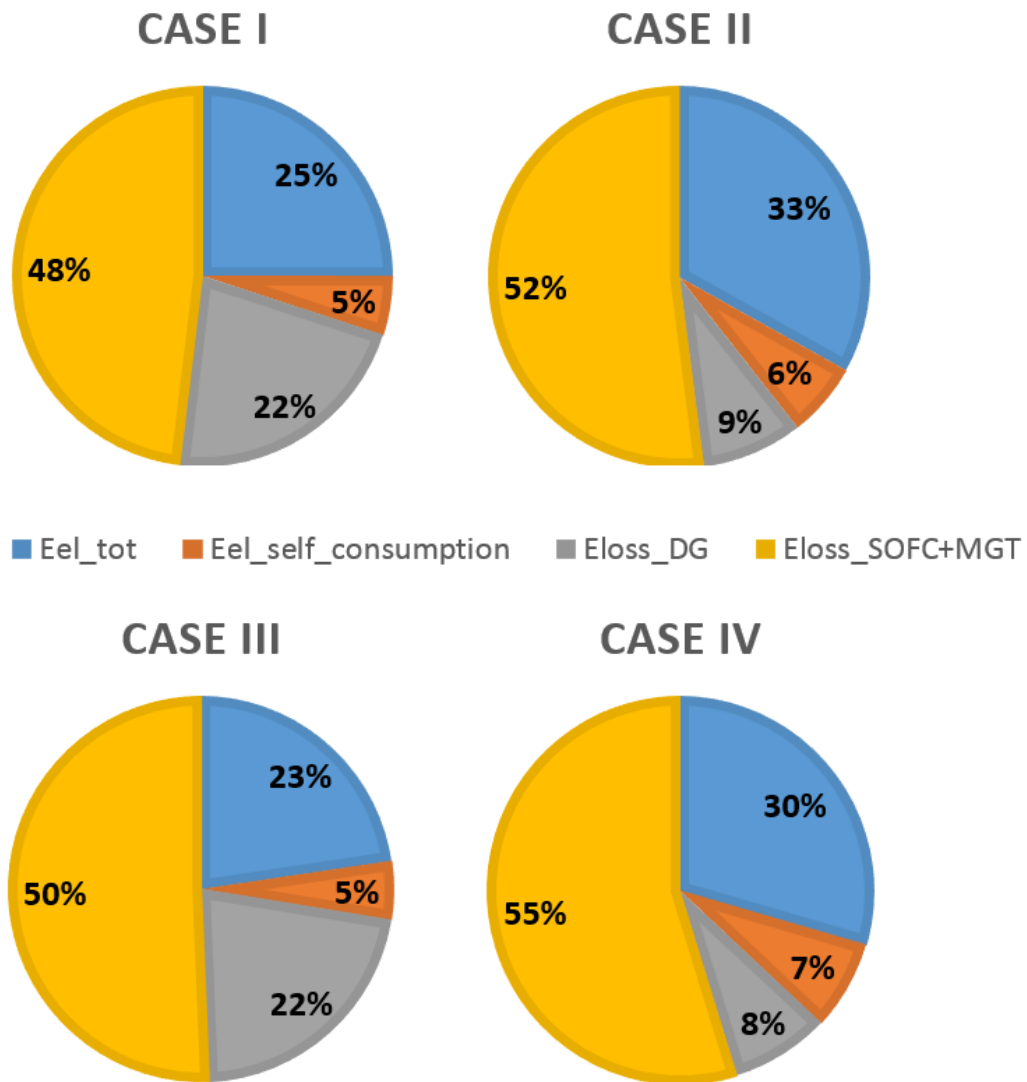


Figure 7: Energy balances of the studied cases

Table 1: Model parameters I

Membranes properties [31]		
Material	Selectivity α [ad]	Oxygen Permeability γ [mol m ⁻² s ⁻¹ bar ⁻¹]
Matrimid	6.7	62.0 x 10 ⁻⁵
PPO	4.7	37.2 x 10 ⁻⁴
PDMS	2.1	39.6 x 10 ⁻²
Poplar wood chips properties [61]		
Description	Symbol	Value
Total moisture	M	10 %
Carbon content (as received)	C_{ar}	41.62 %
Hydrogen content (as received)	H_{ar}	5.30 %
Nitrogen content (as received)	N_{ar}	0.52 %
Oxygen content (as received)	O_{ar}	39.81 %
Ash content	ASH	2.75 %
Higher heating value (dry basis)	HHV_{db}	15.7 MJ/kg
Gasifier model parameters[48]		
Description	Symbol	Value
As received biomass consumption	\dot{m}_{bio}	187 kg/h
Nominal gasifier thermal power	$P_{th,gas}$	800 kW
Initial calculation temperature	T_{in}	900 K
Pressure	p	1 atm
Equivalence ratio	ER	0.335
Gasifier and filters auxiliary consumption	$P_{DG,self}$	12.5 kW
Cyclic operation hours	$h_{operation}$	360 h
Cyclic maintenance hours	$h_{maintenance}$	4 h
Zeolite 5A parameters of adsorption at 303 K [39]		
Component	B [1/kPa]	q_m [mmol/g]
CO_2	0.019500	3.91900
H_2	0.000361	0.54464
N_2	0.000837	2.62543
CH_4	0.002535	2.75403
CO	0.004350	2.75800

Table 2: Model parameters II

Storage and compressor model parameters		
Description	Symbol	Value
Politropic exponent of the syngas [54]	m	1.33
Syngas compressor efficiency [54]	η_{comp}	92 %
Storage tank temperature	T_s	298.15 K
Initial syngas amount in the tanks	n_{in}	$7 * 10^4$ mol
Total tanks volume	V	650 m ³
SOFC model parameters		
Description	Symbol	Value
Fuel utilization factor	U_f	0.85
Recirculation factor	r	0.2
Operating temperature	T_{sofc}	1073.15 K
Anode pressure loss	Δp_a	500 Pa
Cathode pressure loss	Δp_c	1000 Pa
Anode pressure loss	Δp_a	500 Pa
Current density	i	300 mA/cm ²
Active cell area	A_{cell}	81 cm ²
Cells for each stack	$n_{cell,stack}$	75 cells
Number of stacks	n_{stack}	145 stacks
Cathode air excess	$vent$	1.15
Pressure ratio	PR	2.5
Steam to carbon coefficient	STC	1.4
Electrochemical parameters taken from [18]		
MGT model parameters [18]		
Description	Symbol	Value
Politropic exponenet of the air	m	1.33
Turbine isentropic efficiency	$\eta_{is,turb}$	84 %
Air compressor isentropic efficiency	$\eta_{is,comp}$	75 %
Turbine mechanical efficiency	$\eta_{mec,turb}$	99 %
Air compressor mechanical efficiency	$\eta_{mec,comp}$	98 %
Recuperator effectiveness	η_{rec}	85 %
Burner efficiency	$\eta_{eff,burner}$	99 %
MGT generator efficiency	$\eta_{alt,MGT}$	95 %
Pressure ratio	PR	2.5

Table 3: Case I (Gasifier + SOFC + MGT) simulation results

Gasifier		
Description	Symbol	Value
H_2 syngas fraction	x_{H_2}	19.03 %
H_2O syngas fraction	x_{H_2O}	7.78 %
CO syngas fraction	x_{CO}	15.10 %
CH_4 syngas fraction	x_{CH_4}	1.18 %
CO_2 syngas fraction	x_{CO_2}	13.99 %
N_2 syngas fraction	x_{N_2}	42.92 %
Air inlet flow	Q_{air}	2.94 mol/s
Syngas molar flow	\dot{n}_{syngas}	5.01 mol/s
Syngas higher heating value	$HHV_{syngas,db}$	4.75 MJ/Nm ³
Specific volumetric tar production	m_{tar,Nm^3}	23.63 g/Nm ³
Gasifier cold gas efficiency	η_{cold}	78.98 %
Average temperature of gasification	T	895 K
SOFC + MGT		
Description	Symbol	Value
Syngas molar flow to SOFC-MGT unit	\dot{n}_{SOFC}	4.95 mol/s
SOFC electrical power production	P_{SOFC}	136.70 kW
MGT electrical power production	P_{MGT}	60.73 kW
Total SOFC-MGT electrical power production	$P_{SOFC+MGT}$	197.43 kW
SOFC+MGT electrical efficiency	$\eta_{SOFC+MGT}$	37.46 %
Overall system		
Description	Symbol	Value
Storage tank pressure range	p_{serv}	2.67-5.39 bar
Average electrical auxiliary consumption	P_{self}	34.24 kW _{el}
Average electrical total power production	P_{tot}	163.19 kW _{el}
Average total electrical efficiency	η_{tot}	25.43 %

Table 4: Case II (PPO + Gasifier + SOFC + MGT) simulation results

PPO module		
Air inlet flow	Q_{air}	2.97 mol/s
Permeate molar flow	Q_P	1.27 mol/s
Retentate molar flow	Q_R	1.69 mol/s
Molar fraction of O_2 in permeate	y_{O_2}	48.9 %
Molar fraction of N_2 in permeate	y_{N_2}	51.1 %
Electric power consumption	$P_{el,PPO}$	15.3 kW
Gasifier		
Description	Symbol	Value
H_2 syngas fraction	x_{H_2}	28.49 %
H_2O syngas fraction	x_{H_2O}	9.91 %
CO syngas fraction	x_{CO}	26.33 %
CH_4 syngas fraction	x_{CH_4}	1.66 %
CO_2 syngas fraction	x_{CO_2}	17.2 %
N_2 syngas fraction	x_{N_2}	16.41 %
Syngas molar flow	\dot{n}_{syngas}	3.589 mol/s
Syngas higher heating value	$HHV_{syngas,db}$	7.55 MJ/Nm ³
Specific volumetric tar production	m_{tar,Nm^3}	0.27 g/Nm ³
Gasifier cold gas efficiency	η_{cold}	92.0 %
Average temperature of gasification	T	931 K
SOFC + MGT		
Description	Symbol	Value
Syngas molar flow to SOFC-MGT unit	\dot{n}_{SOFC}	3.545 mol/s
SOFC electrical power production	P_{SOFC}	184.20 kW
MGT electrical power production	P_{MGT}	68.33 kW
Total SOFC-MGT electrical power production	$P_{SOFC+MGT}$	252.53 kW
SOFC+MGT electrical efficiency	$\eta_{SOFC+MGT}$	42.08 %
Overall system		
Description	Symbol	Value
Storage tank pressure range	p_{serv}	2.67-4.62 bar
Average electrical auxiliary consumption	P_{self}	42.01 kW _{el}
Average electrical total power production	P_{tot}	210.52 kW _{el}
Average total electrical efficiency	η_{tot}	32.81 %

Table 5: Case III (Gasifier + ZEO + SOFC + MGT) simulation results

Gasifier (see Case I)		
ZEO		
Description	Symbol	Value
H_2 syngas fraction after adsoption	x_{H_2}	25.36 %
CO syngas fraction after adsoption	x_{CO}	17.08 %
CH_4 syngas fraction after adsoption	x_{CH_4}	1.43 %
CO_2 syngas fraction after adsoption	x_{CO_2}	0.39 %
N_2 syngas fraction after adsoption	x_{N_2}	55.73 %
Syngas molar flow after adsoption	\dot{n}_{syngas}	4.065 mol/s
Syngas higher heating value after adsoption	$HHV_{syngas,db}$	5.9 MJ/Nm ³
Active zeolite mass for every regeneration cycle	m_{zeo}	23.742 kg
SOFC + MGT		
Description	Symbol	Value
Syngas molar flow to SOFC-MGT unit	\dot{n}_{SOFC}	4.020 mol/s
SOFC electrical power production	P_{SOFC}	138.50 kW
MGT electrical power production	P_{MGT}	44.00 kW
Total SOFC-MGT electrical power production	$P_{SOFC+MGT}$	182.5 kW
SOFC+MGT electrical efficiency	$\eta_{SOFC+MGT}$	34.33 %
Overall system		
Description	Symbol	Value
Storage tank pressure range	p_{serb}	2.66-4.88 bar
Average electrical auxiliary consumption	P_{self}	33.76 kW _{el}
Average electrical total power production	P_{tot}	148.74 kW _{el}
Average total electrical efficiency	η_{tot}	22.87 %

Table 6: Case IV (PPO + Gasifier + ZEO + SOFC + MGT) simulation results

PPO module (see Case II)		
Gasifier (see Case II)		
ZEO		
Description	Symbol	Value
H_2 syngas fraction after adsorption	x_{H_2}	41.53 %
CO syngas fraction after adsorption	x_{CO}	32.54 %
CH_4 syngas fraction after adsorption	x_{CH_4}	2.21 %
CO_2 syngas fraction after adsorption	x_{CO_2}	0.43 %
N_2 syngas fraction after adsorption	x_{N_2}	23.30 %
Syngas molar flow after adsorption	\dot{n}_{syngas}	2.726 mol/s
Syngas higher heating value after adsorption	$HHV_{syngas,db}$	10.19 MJ/Nm ³
Active zeolite mass for every regeneration cycle	m_{zeo}	20.244 kg
SOFC + MGT		
Description	Symbol	Value
Syngas molar flow to SOFC-MGT unit	\dot{n}_{SOFC}	2.696 mol/s
SOFC electrical power production	P_{SOFC}	184.70 kW
MGT electrical power production	P_{MGT}	51.80 kW
Total SOFC-MGT electrical power production	$P_{SOFC+MGT}$	236.50 kW
SOFC+MGT electrical efficiency	$\eta_{SOFC+MGT}$	38.41 %
Overall system		
Description	Symbol	Value
Storage tank pressure range	p_{serb}	2.66-4.15 bar
Average electrical auxiliary consumption	P_{self}	51.80 kW _{el}
Average electrical total power production	P_{tot}	194.53 kW _{el}
Average total electrical efficiency	η_{tot}	30.32 %

LaTeX Source Files

[Click here to download LaTeX Source Files: Manuscript_ECM_review_august_2016_highlight.tex](#)

LaTeX Source Files

[Click here to download LaTeX Source Files: Manuscript_ECM_review_august_2016_not_highlight.tex](#)

